# Smart charging with demand response and energy peak shaving for reefer containers with Internet-of-Things

Tang, Guolei; Zhao, Zhuoyao; Schulte, Frederik; Iris, Çağatay

**DOI**
10.1080/00207543.2025.2499868

**Publication date**
2025

**Document Version**
Final published version

**Published in**
International Journal of Production Research

**Citation (APA)**
Tang, G., Zhao, Z., Schulte, F., & Iris, Ç. (2025). Smart charging with demand response and energy peak shaving for reefer containers with Internet-of-Things. *International Journal of Production Research*, *63*(20), 7460-7485. https://doi.org/10.1080/00207543.2025.2499868

Taylor & Francis
Taylor & Francis Group

International Journal of Production Research

ISSN: 0020-7543 (Print) 1366-588X (Online) Journal homepage: www.tandfonline.com/journals/tprs20

# Smart charging with demand response and energy peak shaving for reefer containers with Internet-of-Things

Guolei Tang, Zhuoyao Zhao, Frederik Schulte & Çağatay Iris

**To cite this article:** Guolei Tang, Zhuoyao Zhao, Frederik Schulte & Çağatay Iris (2025) Smart charging with demand response and energy peak shaving for reefer containers with Internet-of-Things, International Journal of Production Research, 63:20, 7460-7485, DOI: 10.1080/00207543.2025.2499868

**To link to this article:** https://doi.org/10.1080/00207543.2025.2499868



Published online: 07 May 2025.

INTERNATIONAL JOURNAL OF PRODUCTION RESEARCH
2025, VOL. 63, NO. 20, 7460–7485
https://doi.org/10.1080/00207543.2025.2499868

Taylor & Francis
Taylor & Francis Group



# Smart charging with demand response and energy peak shaving for reefer containers with Internet-of-Things

Guolei Tang[a], Zhuoyao Zhao[a], Frederik Schulte [b] and Çağatay Iris [c]

[a]State Key Laboratory of Coastal and Offshore Engineering, Dalian University of Technology, Dalian, Liaoning, People's Republic of China; [b]Faculty of Mechanical Engineering, Delft University of Technology, Delft, The Netherlands; [c]University of Liverpool Management School, Liverpool, UK

**ABSTRACT**

Port terminals, especially their reefer container yards, face surging power demands. Efficient reefer charging is critical for port sustainability and efficiency, as it helps reduce peak energy loads and total energy consumption. This requires consideration of reefer characteristics, temperature control requirements, time-variant energy prices, port power distribution network and environmental factors such as ambient temperature and sunlight. Optimising the charging power and internal temperature of reefers is therefore essential. This study introduces mathematical models to optimise two efficient charging schemes for reefers: flexible power charging and on/off power charging. Internet-of-Things (IoT) technologies can enable tailored optimisation strategies for reefer charging by facilitating information sharing among reefers and the charging planning system. This study also proposes a cyber-physical system for IoT that allows these charging schemes to be implemented. Using data from existing ports, the results demonstrate that the optimised reefer charging plan significantly reduces energy costs and alleviates peak energy consumption, consistently outperforming the baseline policy. In the optimised plan, charging periods are slightly adjusted based on energy price in each period as part of a demand response strategy, and intermittent charging is actively used for peak energy shaving. The study also quantifies the positive impact of roof shade installation. Findings provide actionable insights for refrigerated goods.

**ARTICLE HISTORY**
Received 20 July 2024
Accepted 13 April 2025

**KEYWORDS**
Industry 4.0 in ports; green port yard management; smart port; charging optimisation; IoT in logistics; energy management optimisation

## 1. Introduction

Refrigerated goods are important energy consumers in warehouse and cold chain operations. Container terminals, whether seaport or inland port, serve as critical transportation hubs with significantly increased electricity demand due to electrification initiatives. The refrigerated or reefer container yard is a major power consumer in ports, accounting for 50% of total energy consumption in many ports (Iris and Lam 2019). Port yards temporarily store refrigerated containers for import, export, or transshipment, ensuring that each reefer container maintains the required temperature range through regular charging. When a large number of reefer containers are charged simultaneously, it can lead to peaks in energy consumption. These peaks put significant stress on the port's power substations and grid connections, resulting in higher electricity costs, as energy charges are partly based on peak power consumption. Moreover, total energy consumption is influenced by charging power decisions in each time period. An efficient charging plan can help reduce total energy consumption, peak energy consumption, and associated costs.

A large number of ports progressively move towards fully electrified operations, moving away from fossil fuel-dependent energy sources. This transition significantly increases the demand for electricity and results in higher peak power loads. Effective peak power shaving and energy demand response policies (i.e. adjusting power demand considering unit electricity price) are therefore essential to prevent excessive power consumption, reduce costs and alleviate pressure on the power distribution infrastructure. Reefers offer a unique opportunity for optimised energy management. Ports such as PSA International and Hongkong International Terminals have introduced reefer monitoring and control systems for similar purposes (Port Technology International 2021; PSA International n.d). These systems enable remote monitoring and control of temperature, humidity, and power management in refrigerated containers through

**CONTACT** Çağatay Iris c.iris@liverpool.ac.uk University of Liverpool Management School, Liverpool L69 7ZH, UK

two-way data communication and automated decision-making. This approach is a crucial step toward developing more efficient, sustainable, and digital ports.

The optimisation of charging power and charging duration for each reefer faces various challenges. First, container terminals handle many reefers, each storing specific products with unique requirements such as temperature range. Second, the dynamic arrivals and departures of reefers at the terminal yard complicates the intermittent charging and demand response strategies. Third, unit electric power purchasing cost fluctuates on an hourly basis, leading to significant variations in the cost of charging throughout the day. The costs of peak energy consumption also affect the total amount of energy charged. Fourth, the existing power distribution network and grid connection specifications in a port limits power charging capacity in a specific way in each time period. Lastly, environmental and weather conditions in each time period greatly affect both the internal temperature of reefers and charging requirements. Factors such as ambient temperature, the availability of yard roof shade and the sunlight exposure influence the cooling and heating requirements of reefers. Charging and temperature management decisions must consider all of these factors, in addition to the energy costing structure, to obtain optimal decisions in each time unit.

The reefer containers management is studied in a limited number of works in the cold chain and port domain and the existing studies do not focus on optimising energy-efficient charging and temperature management of each reefer container (Iris and Lam 2019). Our problem determines the charging power and the internal temperature of each reefer in each time period. A port terminal makes these decisions for a planning horizon (e.g. spanning several days) using discretised time units (e.g. hourly planning, 15-minute planning), taking into account various factors such as reefer container arrival and departure times, reefer temperature requirements, power distribution network characteristics, ambient conditions, energy prices, etc.

Aiming at energy-efficient charging for reefer containers, this paper proposes two smart charging planning methods for reefers under energy demand response and peak shaving: flexible power charging (FPC) and on/off fixed power charging (ON/OFF). In the FPC method, the charging power delivered (decision variable) can take any value within a specific range in each time period. Whereas, the ON/OFF charging method only allows the power to be either ON or OFF, with fixed power values (maximum (ON) or minimum (OFF)) for each mode in each time period. The objective function comprises energy-related costs, which include both the peak energy consumption in the entire planning horizon (i.e. peak cost) and the total energy consumption for each time period (i.e. total hourly energy consumption cost).

The aforementioned charging schemes are enabled by a Cyber-Physical System (CPS), in which sensors detect the condition of reefer containers and actuators enforce optimised charging policies. This system provides the technical network framework and utilises an Internet of Things (IoT) infrastructure. The charging optimisation and temperature control mechanism requires each reefer to have seamless communication with other reefers and with the charging sockets, forming a bi-directional interconnected network. IoT facilitates the integration of cloud services into CPS without requiring human intervention, forming a dynamic global network of interconnected reefers with self-configuring capabilities.

The main contributions are summarised as follows:

- To the best of our knowledge, this is the first work that presents optimisation models to obtain multi-period charging and temperature management decisions for all reefers in a container yard considering different charging methods (flexible power charging and on/off fixed power charging), energy prices (peak prices and time-variant consumption prices), port power distribution network properties, container details and environmental factors.
- This study proposes novel charging policies that leverage technological advancements in CPS for IoT applications to facilitate energy peak load shaving and demand response at reefer yards. These systems transform traditional reefers into intelligent systems capable of remote monitoring and automated power management.
- Our results suggest charging in time periods with lower energy prices, effectively shifting mid-day charging to off-peak hours for demand response (e.g. early-day cooling), while intermittent charging is applied for peak shaving when there are many reefer containers in the yard. Our research also informs port operators about peak power thresholds, which can be incorporated into electricity supplier contracts.
- Findings deliver substantial cost savings and carbon emission reductions through smart power charging and advanced control of FPC and ON/OFF charging schemes, revealing FPC as the better approach. The impact of roof shade cover in the yard is quantified for the first time and the positive impact is shown.

In the subsequent section, we review the state-of-the-art of the literature relevant to our study. In Section 3, the formal problem definition and details of problem specifications are presented. Section 4 introduces mathematical

models for each smart charging and temperature management method. The case study (instances) and numerical results for the instances are presented in Section 5, along with extensive sensitivity analyses and managerial insights. The final section concludes the study and discusses future research directions.

## 2. Literature review

Electrified port equipment and electrified port areas –including cranes, yard vehicles, stacking equipment, reefer racks, and buildings – have led to a surge in port electricity demand. Previous studies confirm that port operations planning can significantly reduce both peak energy costs and total energy consumption costs, primarily due to scheduling flexibility. Energy-aware operations planning is crucial for logistics facilities and manufacturing (Prabhu, Trentesaux, and Taisch 2015). Geerlings, Heij, and van Duin (2018) apply peak shaving concepts to electrified quay crane (QC) operations, limiting the number of cranes lifting containers simultaneously. This operations planning approach prevents excessive simultaneous crane operation, significantly reducing peak energy costs while only slightly decreasing QC handling rates. A 50% reduction in the number of lifting QCs leads to a roughly 40% decrease in peak energy costs. Tang et al. (2020) present a simulation method to assess the impact of two peak shaving policies on the handling rates of QCs and yard trucks (YTs). Their results indicate that synchronising QC and YT operations leads to a reduction in peak energy consumption. Alasali, Haben, and Holderbaum (2019) validate the use of an energy storage system (ESS) integrated into an electrified yard crane (YC). They address the resulting optimal power flow problem using a stochastic control algorithm to minimise idle electrical energy consumption.

Some studies have integrated reefer container yards into the energy management systems of ports. Iris and Lam (2021) present the first port microgrid study that integrates berth, QC, and YC assignments with energy flow decisions to reduce energy costs. Their results highlight the positive contribution of energy demand response in port microgrids. Mao et al. (2022) propose an integrated flexible resource scheduling model that considers berth allocation for cruise ships. In addition to power flows, their study incorporates heat and cooling flows as part of a multi-energy system. However, both Iris and Lam (2021) and Mao et al. (2022) only estimate average energy consumption in the reefer yard. They lack reliable control and decision-making at the individual reefer level and do not optimise detailed reefer charging decisions. In these studies, the reefer container yard is modelled as a single entity with a total energy demand within the energy system. Xiong et al. (2024) treat the energy consumption of refrigerated warehouses as a low-priority load to optimise energy supply planning. Sarantakos et al. (2024) present an optimal operation and power management framework for an electrified port, integrating the planning of cranes, port vehicles, reefer parks, and energy storage. However, none of these studies optimise reefer charging, temperature regulation, or energy management at the individual container level, considering different reefer temperature requirements and ambient conditions, as addressed in this work.

There are studies to estimate the power demand of individual reefer containers using analytical and simulation techniques. Although these studies do not optimise the power charging of reefer containers, they inform about the approximated power demand of reefer containers. Shinoda, Budiyanto, and Sugimura (2022) and Budiyanto et al. (2018) factor in solar radiation and heat conduction on container walls, devising a finite-volume method to calculate reefer power requirements with and without roof shades. Budiyanto, Nasruddin, and Zhafari (2019) predict reefer power consumption by modelling heat transfer processes and heat load. These studies primarily inform about individual reefer power consumption while accounting for solar radiation effects.

Terminal operators have to ensure that the internal temperature of each reefer container is kept in a cargo-specific range. Some studies focus on the temperature and energy management problem of reefers at the yard. van Duin et al. (2018) provide two methods, an intermittent charging approach and a peak-restriction-based charging approach. In intermittent charging, they set charging for each set of containers (rack) for 5 and 15 minutes. For the peak-restriction based method, they charge until the lowest allowed inside temperature is reached. The authors conclude that these approaches have significant opportunities for reefers at the yard, with the aim of reducing peak power demand and total cargo loss rates. Nel, Goedhals-Gerber, and van Dyk (2024) compare the efficacy of two technologies fitted inside reefer containers to improve airflow for table grape shipments. Finally, Moros-Daza et al. (2024) suggest underground storage space for reefer storage and the suggested warehousing system reduces solar radiation and ambient temperature for reefer containers. Results show significant cost savings for reefer power charging, though significant investment might be required for the suggested system.

The charging planning of electric vehicles (EVs) shares several similarities with that of refrigerated containers, particularly in optimising power delivery and management. Key advancements include smart charging algorithms, control strategies, and vehicle-to-grid (V2G) contract design. Lu et al. (2023) review the role of EVs in

seaports, highlighting opportunities for optimising EV charging in these environments. Charging optimisation has received significant attention in road transport (Wang and Chen 2024; Zhang, Zhao, and Hu 2023). Said and Mouftah (2017) present a peak load management technique and a guidance algorithm that coordinates EV charging and discharging to mitigate the negative impact of EV penetration on existing power networks. Aloqaily et al. (2016) propose a flexible charging and discharging algorithm to manage peak-time power demand effectively. EV batteries can serve as backup energy storage, shifting power usage from off-peak to on-peak periods. Alghamdi, Said, and Mouftah (2021) introduce a profit-maximisation model for EV charging and discharging, accounting for electricity price variations throughout the day. Jiao et al. (2022) design a revenue-sharing contract for V2G power dispatching to coordinate multi-party interests in the power supply chain and enhance V2G service adoption.

Furthermore, many researchers study the future role of Machine Learning (ML), Artificial Intelligence (AI), IoT, and blockchain in power management. The development of these technologies is crucial to address the challenges in charging load prediction, decision-making, real-time data transfer and cybersecurity. Sarda et al. (2024) provide a review on the impact and challenges of EVs on the power grids, including increased electricity demand, potential risks to grid quality and safety, and higher power losses. They also discuss AI-driven algorithms for dynamic pricing and charging load prediction, decision-making. Said et al. (2024) and Said (2023) discuss the challenges, solutions, and opportunities associated with demand response, and highlight the critical role of IoT, ML, and blockchain technologies in addressing key cybersecurity and information flow issues. Munusamy and Vairavasundaram (2024) provide a comprehensive review of energy trading and security using blockchain, while also exploring the potential of AI and ML algorithms to enhance sustainable energy management and grid resilience. Khabbouchi et al. (2023) introduce a novel Energy Management Protocol (EMP) that combines ML and game-theoretic algorithms to efficiently manage the charging and discharging processes of EVs, particularly addressing wind power variability. Charpentier et al. (2024) point out that the emergence of 5G offers data rates of up to 20 Gbps, latencies as low as 5 milliseconds (ms) and exceptional reliability. These advancements present a significant opportunity for innovation in the maritime sector, enabling smarter, safer operations and seamless real-time information flow.

## 3. Problem description

We consider a port reefer yard where a total of $I$ reefer containers arrive and depart during a planning horizon of $T$ discrete time periods. The planning horizon is divided into time intervals, with $\Delta T^h$ and $\Delta T^s$ representing the time interval length in hours and in seconds, respectively. Each reefer container $i$ has a minimum required power charging amount ($P_i^{\min}$) and a maximum allowed power charging amount ($P_i^{\max}$) for each time period, along with its expected arrival time into yard ($ETA_i$) and expected departure time from the yard ($ETD_i$). Each container has an initial internal temperature ($U_i^{ini}$), a permissible minimum internal temperature ($U_i^{\min}$) for each time period, a permissible maximum internal temperature ($U_i^{\max}$) for each time period, a surface (wall) area ($A_i$), a thermal insulation factor ($K_i$), the mass ($M_i$), and the specific heat capacity of the cargo stored inside the reefer ($J_i$).

The problem involves determining the amount of power to charge into each reefer and the internal temperature of each reefer at each time step. The charging power decisions determine the charging current in cables connected to every single device in the power distribution network in the port. Additionally, charging power decisions determine peak power consumption. The objective is to minimise total energy costs (i.e. the total energy consumption cost and peak energy consumption cost) by reducing electricity consumption through demand response and peak power shaving.

### 3.1. A cyber-physical system for IoT application for reefer charging

An intelligent reefer container, known as smart reefer, is equipped with advanced technologies such as microprocessors, sensors, communication devices, and automated controllers. These devices enable real-time information flow and allow remote control of power charging to the reefer. Current smart reefer applications are limited to remote data monitoring and visualisation, lacking involvement in energy management.

In traditional reefer yards, port operators manually check and record container temperatures every 4 hours, significantly straining human resources. Our proposed charging optimisation approach determines the power charging and temperature settings of all reefer containers while minimising costs and adhering to constraints. It ensures ideal conditions at discretised 15-minute intervals – an impractical frequency for manual intervention. Automating the charging process is therefore essential to enhance efficiency, enable real-time control, and reduce

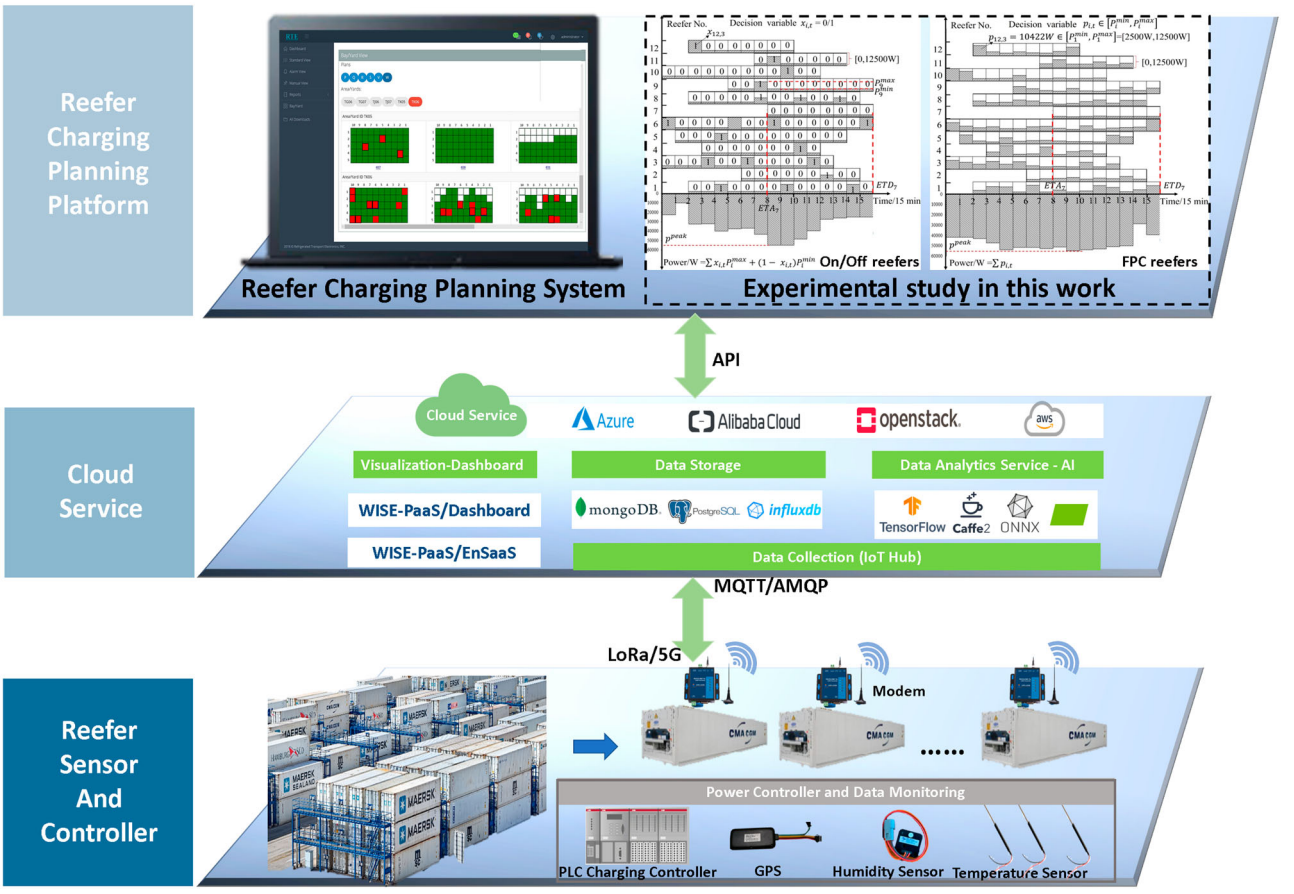


**Figure 1.** Cyber-physical system and IoT of smart reefer yards (Source: Authors).

human resource demands. The integration of CPS and IoT technologies addresses this challenge by enabling signal transmission from the charging planning system, automating power adjustments in real time, and improving operational efficiency. Thus, we propose a CPS and IoT framework for reefer charging based on the remote reefer monitoring and control, as shown in Figure 1.

In Figure 1, the top layer represents the reefer charging planning platform, which serves as the decision-making layer of the cyber-physical system (CPS). Reefer charging planning determines the charging power and temperature for each reefer based on operational requirements. Experimental results in this work (Section 5.2) are based on the top layer of Figure 1. The suggested charging policies can be implemented with remote monitoring and control, enabled by other system layers. The middle layer comprises cloud services, which act as intermediaries for (real-time) data management, storage, and control. The bottom layer functions as the execution and data collection layer which includes the power distribution system, communication systems, sensors, controllers and reefers.

The reefer charging platform (top layer) communicates with the cloud service layer (middle layer) via Application Programming Interfaces (APIs), ensuring efficient data transfer and command execution. The IoT plays a vital role in this system, connecting data from physical devices (reefer sensors and equipment) to reefer charging planning models in the digital space. It enables seamless cloud service integration into the CPS without human intervention and facilitates communication between reefers.

The cloud service layer (middle layer) manages the storage and processing of large data volumes using communication protocols such as MQTT and AMQP. It also ensures reliable, low-latency data transmission via advanced wireless technologies like LoRa and 5G, facilitating real-time adjustments in the reefer park (bottom layer). Programmable Logic Controller (PLC) systems, in the bottom layer, receive power control commands from the reefer charging planning platform through cloud services and the charging physically executes. The bottom layer collects reefer data (temperature, humidity, etc.) and inform upper layers, enabling two-way remote monitoring and control. The power distribution network at a port follows a structured design. Each reefer connects to a charging socket, a batch of sockets links to a distribution box, and multiple distribution boxes connect to a box-type transformer. These components ultimately connect

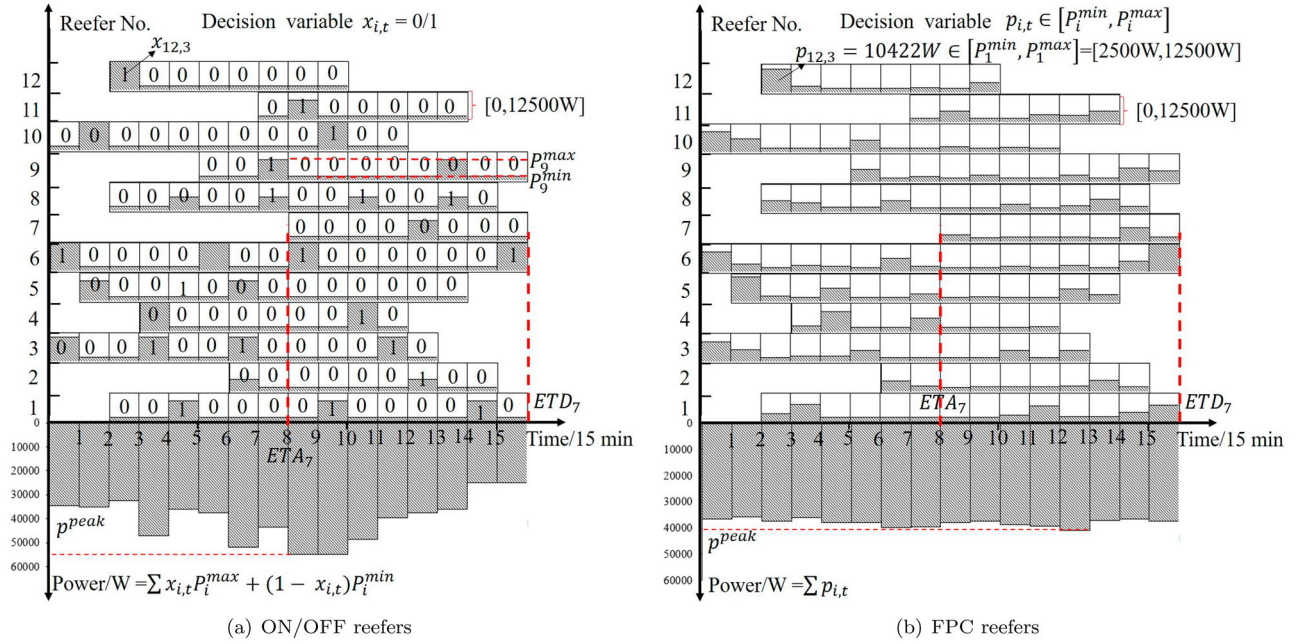


**Figure 2.** Examples of reefer charging solution (For notations refer to Table 1). (a) ON/OFF reefers and (b) FPC reefers.

to a transformer substation box (see, e.g. Figure 3), allowing for different voltage levels across the system.

### 3.2. Reefer charging planning: charging and temperature optimisation problem

The problem decides on power charging amount ($p_{i,t}$) for each reefer in each time unit in the FPC case, and power charging states (ON or OFF, represented as $x_{i,t}$) in ON/OFF case. It also optimises the internal temperature of each reefer in each time unit ($u_{i,t}$) as a function of the internal temperature of the previous period, charging amount in that period, and environmental factors in that period.

The charging decisions determine the power and current flow in the distribution box, the box type transformer and the transformer substation bus since the voltage is an input parameter for each device in the power distribution network. The charging decisions also determine the total energy consumption in each period and the peak power ($p^{peak}$) in the entire planning horizon. These decisions are transmitted to smart reefers via CPS and IoT framework.

The objective function consists of two main costs, namely total energy consumption cost (depending on time-variant unit energy consumption cost) and the peak energy consumption cost. The energy consumption cost for a given period $t$ is calculated by multiplying the power consumption by the unit power purchasing price ($C_t^e$) for this period. The total energy consumption cost over the entire planning horizon is the sum of energy consumption costs for all periods. For the peak consumption cost, three different methods are considered:

*Costing based on peak consumption value*: In this method, the port is charged based on the peak consumption ($p^{peak}$) multiplied by the peak price ($C^{p1}$).

*Costing based on both peak consumption value and excess charging beyond the peak consumption threshold*: In this method, the grid (power supplier) sets a peak threshold value ($P^{thr}$) in advance in the contract. The port is charg ed on two peak related costs. The peak power exceeding the threshold is charged at $C^{p3}$, while peak power below the threshold is charged at the normal peak price ($C^{p2}$).

*Costing based on only excess charging beyond the peak consumption threshold*: In this method, the grid (power supplier) sets a peak threshold value ($P^{thr}$) in advance, as specified in the contract. The port is charged only for peak power consumption exceeding the peak threshold at the peak excess price ($C^{p4}$).

In the reefer charging and temperature optimisation problem, we focus on optimal charging planning for demand response and peak shaving based on two charging policies. An example solution in the form of a time-power diagram is shown in Figure 2. In Figure 2, the $x$-axis represents discretised time, the upper $y$-axis presents the indexes of the reefer containers, and the lower $y$-axis shows the total power consumption in each period. Each reefer is represented by a rectangle, with its left edge showing the arrival, its right edge showing departure times, and its filling as the charging state. The $x$-axis marks the arrival time ($ETA_i$) and departure time ($ETD_i$)

for each reefer. Within the rectangle, each small square represents the charging state of the reefer at each time unit. For ON/OFF charging scheme in Figure 2(a), the charging state is determined by a binary variable ($x_{i,t}$) in Figure 2(a). For a reefer in the yard, if the reefer $i$ is in ON mode during a period ($x_{i,t} = 1$), it receives the maximum charging power ($P_i^{\max}$), otherwise it receives the minimum charging power ($P_i^{\min}$). Power is not provided if the reefer is not stored in the yard. For FPC charging scheme, the problem determines the charging power value ($p_{i,t}$) within the power range in Figure 2(b).

In sub Figure 2(a,b), the total power consumption in the yard at each time unit is represented as column graphs below the horizontal axis. The maximum power consumption over the entire planning horizon is the peak power consumption ($p^{peak}$), for which fees are charged by the grid operator. Each reefer has an upper and lower limit of its internal temperature. The problem aims to determine the power charging amount of each reefer in such a way that reduces peak costs and time-varying energy costs, while keeping the inside temperature within the permissible range under environmental considerations and obeying the capacity constraints of the energy infrastructure.

To compare efficiency of our optimisation framework, we present base case policy, commonly used in ports.

*Base Case Policy*: When the internal temperature of the reefer is within the allowed range of the set temperature, auxiliary power is used. Once the internal temperature of the reefer reaches upper temperature bound, charging power is used to cool the reefer down until it reaches lower temperature bound.

## 4. Mathematical models

In this section, we describe six mathematical models for ON/OFF and FPC type charging considering three peak costing schemes. The notations for sets, parameters and variables can be found in Table 1.

### 4.1. ON/OFF charging scheme

We propose a mixed-integer linear programming (MILP) model for ON/OFF reefers charging scheme. The decision variable for charging in ON/OFF case is a binary variable $x_{i,t}$ that determines the ON or OFF mode of each reefer in each time period. The objective function consists of the energy consumption costs and the peak energy costs. The last term in each objective function minimises total energy consumption cost ($\sum_{t\in\mathbf{T}} C_t^e \Delta T^h \psi_t$) for demand response management with time-variant

**Table 1.** Notation for sets, parameters and variables.

| | | |
|---|---|---|
| Sets | | |
| $\mathbf{T}$ | | Set of time periods, $t \in \mathbf{T} = \{0, 1, 2, \ldots, T\}$ |
| $\mathbf{I}$ | | Set of reefers that arrive at yard over the entire planning period, $i \in \mathbf{I} = \{1, 2, \ldots, I\}$ |
| $\mathbf{I}_d$ | | Set of reefers that charged at the distribution box $d$, $\mathbf{I}_d \subset \mathbf{I}$ |
| $\mathbf{I}_{d,t}$ | | Set of reefers that are at the yard in time period $t$ and are charged at the distribution box $d$ |
| $\mathbf{D}$ | | Set of all distribution boxes, $d \in \mathbf{D} = \{1, 2, \ldots, D\}$ |
| $\mathbf{D}_b$ | | Set of distribution box that connected with the reefer box type transformer $b$, $\mathbf{D}_b \subset \mathbf{D}$ |
| $\mathbf{B}$ | | Set of reefer box type transformers, $b \in \mathbf{B} = \{1, 2, \ldots, B\}$ |
| Parameters | | |
| $C_t^e$ | SGD/kWh | Utility grid electricity purchasing price in time period $t$ |
| $C^{p1}$ | SGD/kW | Peak price for costing based on peak consumption value |
| $C^{p2}$ | SGD/kW | Peak price for costing based on both peak consumption value and excess charging beyond the peak consumption threshold |
| $C^{p3}$ | SGD/kW | Peak price for exceeding peak threshold in costing based on both peak consumption value and excess charging beyond the peak consumption threshold |
| $C^{p4}$ | SGD/kW | Peak price for costing based on only excess charging beyond the peak consumption threshold |
| $\Delta T^h$ | h | time interval, time unit is hours, e.g. if time interval is 15 min, $\Delta T^h = 0.25$ |
| $\Delta T^s$ | s | time interval, time unit is seconds, e.g. if time interval is 15 min, $\Delta T^s = 900$ |
| $P_i^{\min}$ | kW | The minimum power for reefer $i$, generally equal to auxiliary power |
| $P_i^{\max}$ | kW | The maximum power for reefer $i$ |
| $P^{thr}$ | kW | The threshold value of peak power |
| $ETA_i$ | | The expected arrival time of reefer $i$ at yard |
| $ETD_i$ | | The expected departure time of reefer $i$ from yard |
| $U_i^{ini}$ | °C | The initial temperature of reefer $i$ when arriving at yard |
| $U_i^{\min}$ | °C | The allowed minimum temperature of reefer $i$ |
| $U_i^{\max}$ | °C | The allowed maximum temperature of reefer $i$ |
| $U_t^{amb}$ | °C | The ambient temperature in time period $t$ |
| $S_t$ | | The sun intensity in time period $t$ |
| $\xi$ | | The heating compensation coefficient |
| $A_i$ | $m^2$ | The surface area of reefer $i$ |
| $K_i$ | $W/m^2.°C$ | The thermal insulation of reefer $i$ |
| $M_i$ | kg | The mass of cargo in reefer $i$ |
| $J_i$ | J/kg·°C | The specific heat of cargo in reefer $i$ |
| $cos\phi$ | | Power to current conversion factor for voltage, which generally is 0.8 |
| $\overline{V}_i, \overline{V}_d, \overline{V}_b$ | V | The voltage of reefer $i$, distribution box $d$ and reefer box type transformer $b$ |
| $I_i^{\max}, I_d^{\max}, I_b^{\max}$ | A | The maximum current of the cable connected with reefer $i$, distribution box $d$ and reefer box type transformer $b$ |

(*continued*).

**Table 1.** Continued.

| | | |
|---|---|---|
| $q_d^{\max}, g_b^{\max}, \psi^{\max}$ | kW | The maximum power capacity of distribution box $d$, reefer box type transformer $b$ and the transformer substation bus, respectively |
| Decision variables for On/off reefers scheme | | |
| $x_{i,t} \in \mathbb{B}$ | | binary, the decision variable for ON/OFF reefer: 1 if reefer $i$ in time period $t$ is ON mode, 0 otherwise |
| Decision variables for FPC reefers scheme | | |
| $p_{i,t} \in \mathbb{R}^+$ | kW | continuous, for FPC reefers: the charging power amount for reefer $i$ in time period $t$ |
| Decision variables for both schemes | | |
| $p^{peak} \in \mathbb{R}^+$ | kW | continuous, the peak power consumption at reefer yard in the planning horizon |
| $u_{i,t} \in \mathbb{R}$ | °C | continuous, the internal temperature of reefer $i$ in time period $t$ |
| $q_{d,t}, g_{b,t}, \psi_t \in \mathbb{R}^+$ | kW | continuous, the power of distribution box $d$, reefer box type transformer $b$ and the transformer substation bus, in time period $t$ |
| $l_{i,t}, l_{d,t}, l_{b,t} \in \mathbb{R}^+$ | A | continuous, the charging current connected with reefer $i$, distribution box $b$ and reefer box type transformer $d$, in time period $t$ |

energy prices. The other terms of the objective functions (1)–(3) minimise peak energy cost in three different peak costing approaches. The mathematical models are presented below.

The objective function for peak power costing based on peak consumption value and total energy consumption is:

$$\min p^{peak} C^{p1} + \sum_{t \in \mathbf{T}} C_t^e \Delta T^h \psi_t \tag{1}$$

The objective function for peak power costing based on both peak consumption value and excess charging beyond the peak threshold, and total energy consumption is:

$$\min C^{p2} p^{peak} + C^{p3} (p^{peak} - P^{thr})^+ + \sum_{t \in \mathbf{T}} C_t^e \Delta T^h \psi_t \tag{2}$$

The objective function for peak power costing based on only excess charging beyond peak threshold, and total energy consumption is:

$$\min C^{p4} (p^{peak} - P^{thr})^+ + \sum_{t \in \mathbf{T}} C_t^e \Delta T^h \psi_t \tag{3}$$

subject to:

$$u_{i,ETA_i} = U_i^{ini}, \quad \forall\, i \in \mathbf{I} \tag{4}$$

$$U_i^{\min} \le u_{i,t} \le U_i^{\max}, \quad \forall\, i \in \mathbf{I}, \forall\, t \in \mathbf{T} : ETA_i < t \le ETD_i \tag{5}$$

$$u_{i,t} = u_{i,t-1} + (U_t^{amb} - u_{i,t-1}) \left(1 - e^{\frac{-\xi A_i K_i (1+S_t) \Delta T^s}{M_i J_i}}\right) - \frac{x_{i,t} P_i^{\max} \Delta T^s}{M_i J_i}, \quad \forall\, i \in \mathbf{I}, \forall\, t \in \mathbf{T} \backslash \{\mathbf{0}\} : ETA_i < t \le ETD_i \tag{6}$$

$$q_{d,t} = \sum_{i \in \mathbf{I}_{d,t}} (x_{i,t} P_i^{\max} + (1 - x_{i,t}) P_i^{\min}), \quad \forall\, d \in \mathbf{D}, \forall\, t \in \mathbf{T} \tag{7}$$

$$g_{b,t} = \sum_{d \in \mathbf{D}_b} q_{d,t}, \quad \forall\, b \in \mathbf{B}, \forall\, t \in \mathbf{T} \tag{8}$$

$$\psi_t = \sum_{b \in \mathbf{B}} g_{b,t}, \quad \forall\, t \in \mathbf{T} \tag{9}$$

$$q_{d,t} \le q_d^{\max}, \quad \forall\, d \in \mathbf{D}, \forall\, t \in \mathbf{T} \tag{10}$$

$$g_{b,t} \le g_b^{\max}, \quad \forall\, b \in \mathbf{B}, \forall\, t \in \mathbf{T} \tag{11}$$

$$\psi_t \le \psi^{\max}, \quad \forall\, t \in \mathbf{T} \tag{12}$$

$$p_{peak} \ge \psi_t, \quad \forall\, t \in \mathbf{T} \tag{13}$$

$$l_{i,t} = \frac{p_{i,t}}{\sqrt{3} \cos\phi \overline{V}_i} \le l_i^{\max}, \quad \forall\, i \in \mathbf{I}_d, \forall\, d \in \mathbf{D}, \forall\, t \in \mathbf{T} \tag{14}$$

$$l_{d,t} = \frac{q_{d,t}}{\sqrt{3} \cos\phi \overline{V}_d} \le l_d^{\max}, \quad \forall\, d \in \mathbf{D}, \forall\, t \in \mathbf{T} \tag{15}$$

$$l_{b,t} = \frac{g_{b,t}}{\sqrt{3} \cos\phi \overline{V}_b} \le l_b^{\max}, \quad \forall\, b \in \mathbf{B}, \forall\, t \in \mathbf{T} \tag{16}$$

$$x_{i,t} = 0, \quad \forall\, i \in \mathbf{I}, \forall\, t \in \mathbf{T} : t > ETD_i \| t \le ETA_i \tag{17}$$

$$x_{i,t} \in \{0, 1\}, \quad \forall\, i \in \mathbf{I}, \forall\, t \in \mathbf{T} \tag{18}$$

$$u_{i,t} \in \mathbb{R}, \quad \forall\, i \in \mathbf{I}, \forall\, t \in \mathbf{T} \tag{19}$$

$$p_{peak} \ge 0 \tag{20}$$

$$l_{i,t} \ge 0, l_{d,t} \ge 0, l_{b,t} \ge 0, \quad \forall\, i \in \mathbf{I}, \forall\, d \in \mathbf{D}, \forall\, b \in \mathbf{B}, \forall\, t \in \mathbf{T} \tag{21}$$

$$q_{d,t} \ge 0, g_{b,t} \ge 0, \psi_t \ge 0, \quad \forall\, d \in \mathbf{D}, \forall\, b \in \mathbf{B}, \forall\, t \in \mathbf{T} \tag{22}$$

The model is subject to the following set of constraints. Constraints (4)–(6) are related to the temperature management of reefers. Constraint (4) sets the temperature of the reefer upon arrival as its initial temperature. Constraint (5) ensures that the temperature of each reefer remains within the permissible range in each time period when it is at the yard. Constraint (6) describes the relationship between temperatures in two consecutive periods and calculates the inside temperature for each period, as referenced in van Duin et al. (2018). The inside temperature in a given period is determined by adding the temperature change during that period to the temperature of the previous period. The temperature change, represented by the second term on the right-hand side of constraint (6), depends on several factors, such as the

surface area of reefer, the thermal insulation of reefer, the mass and heat of the cargo in reefer, as well as the ambient temperature and the sun intensity during the period. This term is used to calculate the temperature change in the absence of power supply. The last term on the right-hand side is used to calculate the temperature decrease when cooling power ($P_i^{\max}$) is supplied. A similar constraint to (6) for period 0, using $U_i^{ini}$ instead of $u_{i,t-1}$, is also included. Constraints (7)–(16) are related to the power and current limits of power distribution network at reefer yard, as shown in Figure 3. To maintain the system's stability, each distribution box and transformer is designed with capacity limits to prevent any component from being overloaded. This ensures that the entire power distribution network operates within safe parameters, providing a reliable power source for the reefers at the terminal. Constraint (7) calculates the power consumption of reefers connected with distribution box $b$ in each period. If it is in ON mode, it gets power of $P_i^{\max}$. If a reefer stored in the yard is in OFF mode, charging power is the value of $P_i^{\min}$. Constraint (8) calculates the power of each reefer box type transformer. Constraint (9) calculates the power of the transformer substation, representing the total power for the entire reefer yard. Constraints (10)–(12) ensure that power usage does not exceed the capacity of the power network infrastructure at port. Constraint (13) sets the maximum total power supplied by the transformer substation over the entire planning horizon as the peak power. Constraints (14)–(16) ensure that the current flowing through each device does not exceed its capacity. The standard power law formulas (Power = Voltage∗Current) are used for current-voltage-power conversion in (14)–(16), assuming that the voltage is a parameter. Constraint (17) indicates that, a reefer will be in OFF mode during periods when a reefer is not stored in the yard. Constraints (18)–(22) set the domains of decision variables.

### 4.2. Flexible power charging scheme

We propose a linear programming (LP) model for flexible power reefers charging scheme. The decision variable $p_{i,t}$ in flexible power charging scheme is continuous and it determines the cooling power delivered to each reefer in each time period. The three different objectives of flexible power charging scheme are presented below.

The objective function for peak power costing based on peak consumption value and total energy consumption is:

$$\min p^{peak} C^{p1} + \sum_{t \in \mathbf{T}} C_t^e \Delta T^h \psi_t \tag{23}$$

The objective function for peak power costing based on both peak consumption value and excess charging beyond peak threshold and total energy consumption is:

$$\min C^{p2} p^{peak} + C^{p3} (p^{peak} - P^{thr})^+ + \sum_{t \in \mathbf{T}} C_t^e \Delta T^h \psi_t \tag{24}$$

The objective function for peak power costing based on only excess charging beyond peak threshold and total energy consumption is:

$$\min C^{p4} (p^{peak} - P^{thr})^+ + \sum_{t \in \mathbf{T}} C_t^e \Delta T^h \psi_t \tag{25}$$

subject to:

$$(4)--(5),\ (8)--(16),\ (19)--(22)$$

$$u_{i,t} = u_{i,t-1} + (U_t^{amb} - u_{i,t-1}) \left(1 - e^{\frac{-\xi A_i K_i (1+S_t) \Delta T^s}{M_i J_i}}\right) - \frac{p_{i,t} \Delta T^s}{M_i J_i}, \forall\, i \in \mathbf{I},\ \forall\, t \in \mathbf{T} \backslash \{\mathbf{0}\} : ETA_i < t \leq ETD_i \tag{26}$$

$$P_i^{\min} \leq p_{i,t} \leq P_i^{\max}, \quad \forall\, i \in \mathbf{I},\ \forall\, t \in \mathbf{T} : ETA_i < t \leq ETD_i \tag{27}$$

$$p_{i,t} = 0, \quad \forall\, i \in \mathbf{I},\ \forall\, t \in \mathbf{T} : t > ETD_i \| t \leq ETA_i \tag{28}$$

$$q_{d,t} = \sum_{i \in \mathbf{I}_{d,t}} p_{i,t}, \quad \forall\, d \in \mathbf{D},\ \forall\, t \in \mathbf{T} \tag{29}$$

$$p_{i,t} \geq 0, \quad \forall\, i \in \mathbf{I},\ \forall\, t \in \mathbf{T} \tag{30}$$

The model inherits constraints (4)–(5) that manage temperature properties, constraints (8)–(16) that restrict the power and current in grid distribution network at reefer yard, and constraints (19)–(22) that set the domain of decision variables. Constraint (26) links temperature decisions to power decisions, similar to constraint (6). Constraint (27) guarantees that the charging power remains within the permissible range. Constraint (28) indicates that the power is not delivered to a reefer in a period in which it is not stored in the yard. Constraint (29) determines the reefer power supplied by each distribution box. Constraint (30) sets the domain of continuous power decisions.

## 5. Case studies and numerical results

This section explains a series of experimental case studies based on a real-world port data. The mathematical models are solved using the IBM CPLEX 12.10 with a default configuration on a computer with a 2.50 GHz processor and 16 GB of RAM. Detailed parameters for the case studies are provided and the numerical results are discussed.

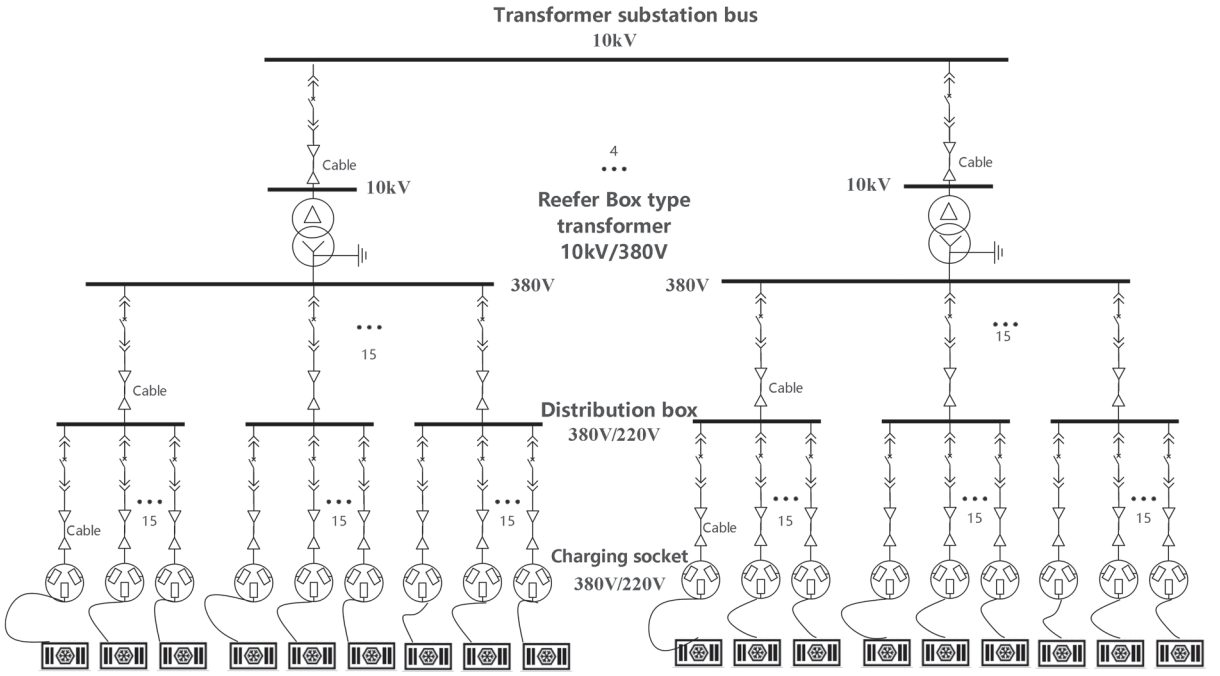


**Figure 3.** Power distribution network infrastructure at the reefer yard.

### 5.1. Instance generation and experimental settings

This section outlines the details of instances including, the number of reefer containers, the reefer yard configurations, attributes of the reefers, the power distribution network, the ambient temperature, the sun intensity and energy price.

#### 5.1.1. Power distribution network at reefer yard

Figure 3 shows the power distribution network in the reefer yard at a real-world container terminal. It is designed to efficiently and safely deliver electricity to reefers, ensuring that each container receives the required power. The network has a substation that distributes power through four box transformers. These four box transformers step down the 10 kV high-voltage power (from the substation) to 380 V, which is the voltage used by the reefers. Each transformer is connected to 15 distribution boxes, which in turn provide power to up to 15 sockets, and each socket serves a single reefer. Each charging socket, distribution box, box transformer, cable, and miniature circuit breaker has specific power and current capacity limits.

#### 5.1.2. Port data and experimental settings

We use realistic port data to generate our instances. The average daily reefer throughput in different container terminals at the Port of Rotterdam is roughly between 100 TEU and 1100 TEU. The number of reefer plugs at container terminals in the Port of Rotterdam ranges between 40 and 3600 (International Institute of Refrigeration 2022; Port Of Rotterdam 2021). In the Port of Antwerp, the average daily reefer throughput is roughly between 300 TEU and 1000 TEU in different terminals (Port of Antwerp n.d).

Thus, we generated four families of random instances (S1–S4: 100, 250, 500, and 1000 reefers) to represent different levels of reefer container throughput over a single day. These instances are randomly generated and represent a range of typical real-world terminal sizes. Detailed information on the total number of reefers in the yard, along with the arrival and departure throughput of the reefers over time, can be found in Figure 4. Both mathematical models are formulated to discretise time into equal intervals, such as 15 minutes. These discretised time units are used to model the problem. The planning horizon spans one day, with energy prices specified on an hourly basis.

#### 5.1.3. Reefer and environmental parameters

Each reefer container stores a single product type from one of the following categories: Deep-Frozen, Frozen, Chilled, Pharmaceuticals, Bananas, Musical Instruments, and Painting Products. For products within the same category, the inside temperature must be within the specified range in Table 2. The specific parameters for each type of product are detailed in Table 2 and are based on the data presented in van Duin et al. (2018). Each reefer holds a specific product and it is known. Each reefer's

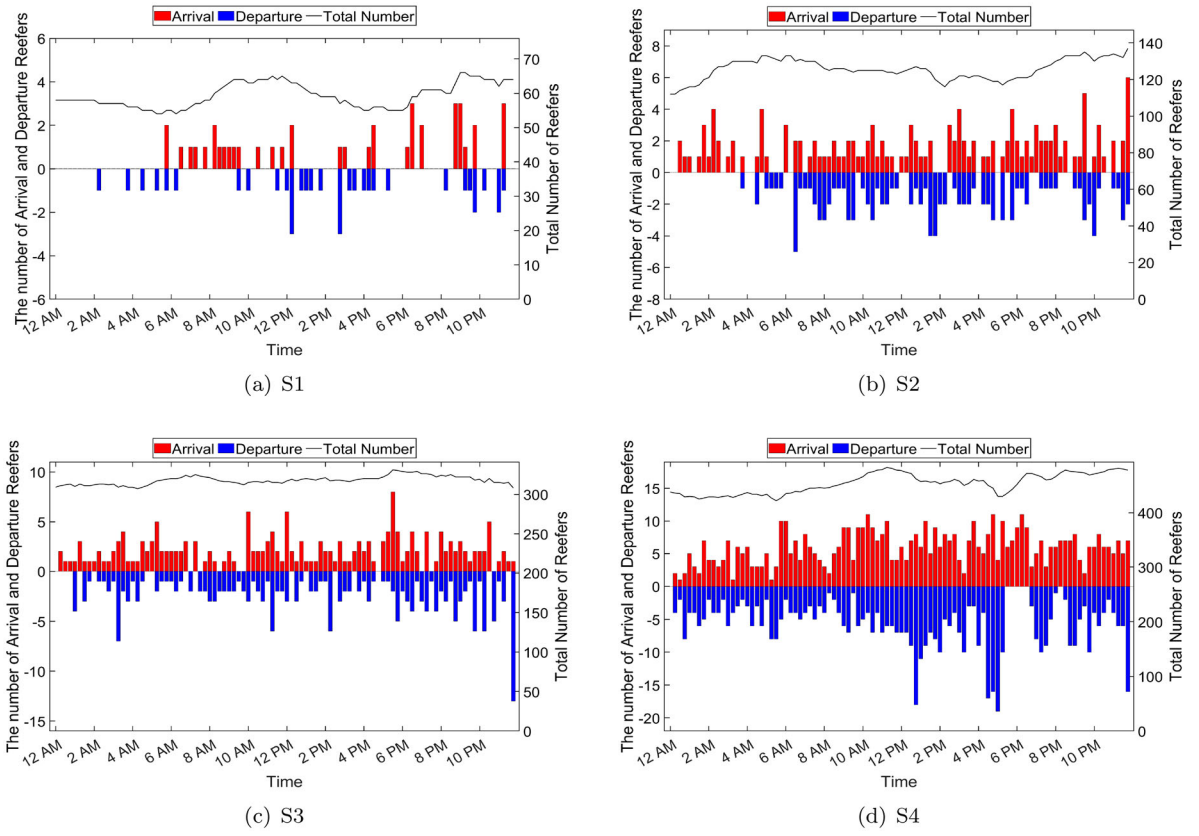


**Figure 4.** The number of reefers at each time unit at container yard in each instance (S1, S2, S3, S4). (a) S1. (b) S2. (c) S3 and (d) S4.

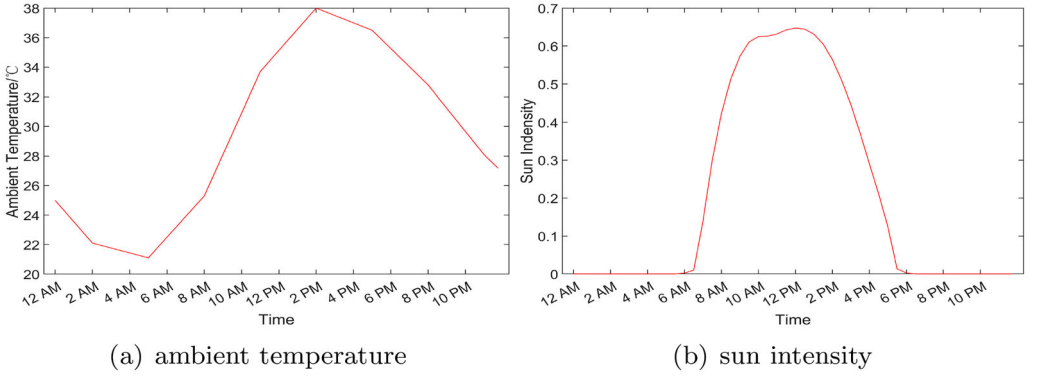


**Figure 5.** Environmental parameters settings. (a) ambient temperature and (b) sun intensity.

actual permissible temperature range is randomly generated by obeying the overall interval of temperature range and using the fluctuation sensitivity in Table 2. Maximum cooling power ($P_i^{\max}$) and auxiliary power for each product are also presented in Table 2. We use the historical data in Budiyanto and Shinoda (2017) to set the ambient temperature and sun intensity, as illustrated in Figure 5. In Figure 6, we present time-variant (hourly) power purchasing price from the grid during one day (day-ahead price), obtained from Iris and Lam (2021).

### 5.2. Experimental results

We first analyze the computational time required to obtain the optimal solution and optimality gap for all instances with different objective functions and charging schemes, then assess the cost and energy profile of obtained solutions. We also investigate the impact of energy peak-shaving, energy demand response, reefer charging rates, temperature management, and the influence of the power distribution network on results.

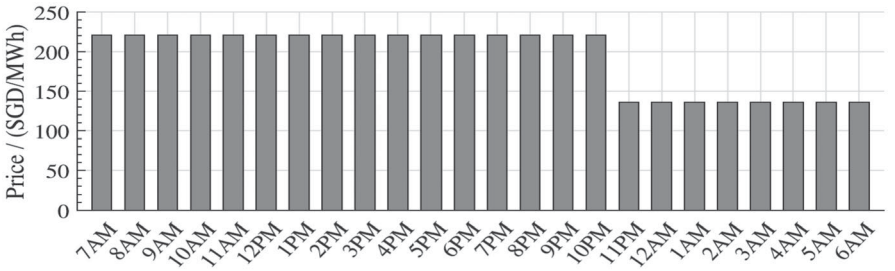


**Figure 6.** Time-of-use energy price, Source: Iris and Lam (2021).

**Table 2.** Reefer cargo classification and the requirements of temperature and power for each cargo (Source from van Duin et al. 2018).

| Product | The overall interval of inside temperature (°C) | Temperature fluctuation sensitivity (°C) | Maximum cooling power (W) | Auxiliary power (W) |
|---|---|---|---|---|
| Deep-Frozen: Seafood, Ice-cream | [−30, −28] | 2 | 5000 | 2500 |
| Frozen: Frozen fish, meat | [−20, −16] | 2 | 6000 | 2500 |
| Chilled: Fruits and Vegetables | [−5, 5] | 1 | 10, 000 | 2500 |
| Pharmaceuticas | [2, 8] | 1 | 10, 000 | 2500 |
| Bananas | 13 | 1 | 12, 000 | 2500 |
| Musical instruments, paintings | [18, 21] | 2 | 15, 000 | 2500 |

**Table 3.** Solution time and optimality gap under different charging schemes and peak thresholds.

| | | Peak costing based on peak consumption (CP) | | | | Peak costing for both peak value and excess charging (CPaEPT) | | | | Peak costing based on excess charging beyond peak threshold (CEPT) | | | |
|---|---|---|---|---|---|---|---|---|---|---|---|---|---|
| | | ON/OFF | | FPC | | ON/OFF | | FPC | | ON/OFF | | FPC | |
| Instances # of reefers | Peak threshold | Time (s) | Gap (%) | Time (s) | Gap (%) | Time (s) | Gap (%) | Time (s) | Gap (%) | Time (s) | Gap (%) | Time (s) | Gap (%) |
| S1 100 | 150 kw | 1800 | 0.81 | 1.21 | 0 | 1800 | 1.02 | 1.15 | 0 | 1800 | 1.11 | 1.18 | 0 |
| | 250 kw | | | | | 1800 | 0.90 | 1.09 | 0 | 1800 | 0.79 | 1.05 | 0 |
| | 350 kw | | | | | 1800 | 0.85 | 1.07 | 0 | 1800 | 0.77 | 1.01 | 0 |
| S2 250 | 400 kw | 1800 | 0.85 | 1.57 | 0 | 1800 | 1.27 | 1.73 | 0 | 1800 | 1.46 | 1.48 | 0 |
| | 550 kw | | | | | 1800 | 1.25 | 1.66 | 0 | 1800 | 0.82 | 1.38 | 0 |
| | 700 kw | | | | | 1800 | 0.95 | 1.69 | 0 | 1800 | 0.89 | 1.57 | 0 |
| S3 500 | 1000 kw | 1800 | 1.02 | 1.84 | 0 | 1800 | 1.54 | 1.95 | 0 | 1800 | 1.55 | 2.04 | 0 |
| | 1500 kw | | | | | 1800 | 1.48 | 1.87 | 0 | 1800 | 0.96 | 1.91 | 0 |
| | 2000 kw | | | | | 1800 | 1.12 | 2.14 | 0 | 1800 | 1.07 | 1.99 | 0 |
| S4 1000 | 1500 kw | 1800 | 1.26 | 2.26 | 0 | 1800 | 1.72 | 2.45 | 0 | 1800 | 2.17 | 2.38 | 0 |
| | 2000 kw | | | | | 1800 | 1.56 | 2.51 | 0 | 1800 | 1.15 | 2.35 | 0 |
| | 3000 kw | | | | | 1800 | 1.32 | 2.69 | 0 | 1800 | 1.13 | 2.71 | 0 |

#### *5.2.1. Model efficiency results*

The models are run with 1800 seconds (30 minutes) of time limit using CPLEX 12.10. Table 3 provides a comprehensive overview of solution time (in seconds) and optimality gap (Gap, %) for all instances. We tested three methods for calculating peak costs: (1) peak costing based on peak consumption (CP), (2) peak costing for both peak value and excess charging (CPaEPT), and (3) peak costing based on excess charging beyond the peak threshold (CEPT). These methods were applied to four different instances (S1–S4) with three distinct peak threshold values (High, Medium, and Low), considering FPC and On/off charging. For FPC charging model, the optimal solution is obtained in less than 3 seconds for all instances. The optimisation model for ON/OFF charging is solved with an average optimality gap of 1.17% within the 30-minute time limit across instances, with 0.98% for CP, 1.24% for CPaEPT and 1.15% for CEPT, respectively. The ON/OFF charging scheme is more challenging to solve to optimality due to the large number of binary variables.

#### *5.2.2. Cost and environmental impact of energy demand response and peak-shaving*

We evaluate the costs and environmental impact of smart charging management for different types of charging schemes. Table 4 displays the results for each experiment, including peak power, total energy demand, peak power cost, energy consumption cost, and carbon emissions. It also highlights the cost savings and emission reductions associated with the three peak cost methods for S1–S4 instances of smart charging management compared to the base case of traditional reefer yards. The optimisation model proposed in this paper

**Table 4.** Energy demand, power cost and carbon emission.

| | Charging scheme | Costing method | $P^{thr}$ (kW) | $p_{peak}$ (kW) | $\Delta P^{+}$ (kW) | Energy (kWh) | cost (SGD) | | | | Carbon emission (kg) | |
|---|---|---|---|---|---|---|---|---|---|---|---|---|
| | | | | | | | Peak | Energy | Total | Saving | Total | Reduction |
| S1 | Base Case Policy | | – | 438.00 | – | 6979.63 | 0.00 | 1407.13 | – | – | 3980.48 | – |
| | ON/ OFF | CP | – | 282.50 | – | 5401.37 | 56.59 | 1013.86 | 1070.46 | 424.42 | 3080.40 | 900.08 |
| | | CPaEPT | 150 | 245.50 | 95.50 | 5385.88 | 87.45 | 1030.43 | 1117.88 | 492.39 | 3071.56 | 908.92 |
| | | | 250 | 252.00 | 2.00 | 5387.38 | 51.29 | 1026.80 | 1078.09 | 492.11 | 3072.42 | 908.06 |
| | | | 350 | 282.50 | 0.00 | 5398.87 | 56.59 | 1013.39 | 1069.99 | 427.29 | 3078.98 | 901.50 |
| | | CEPT | 150 | 229.00 | 79.00 | 5383.87 | 104.66 | 1038.99 | 1143.65 | 645.02 | 3070.42 | 910.06 |
| | | | 250 | 250.50 | 0.50 | 5389.87 | 0.66 | 1027.41 | 1028.07 | 628.12 | 3073.85 | 906.63 |
| | | | 350 | 315.50 | 0.00 | 5403.87 | 0.00 | 1012.79 | 1012.79 | 394.34 | 3081.83 | 898.65 |
| | FPC | CP | – | 282.76 | – | 5345.04 | 56.65 | 999.36 | 1056.01 | 438.87 | 3048.28 | 932.20 |
| | | CPaEPT | 150 | 232.51 | 82.51 | 5322.35 | 79.64 | 1022.11 | 1101.75 | 508.52 | 3035.34 | 945.14 |
| | | | 250 | 250.00 | 0.00 | 5330.92 | 0.00 | 1013.95 | 1013.95 | 556.25 | 3040.22 | 940.26 |
| | | | 350 | 282.75 | 0.00 | 5345.03 | 56.64 | 999.37 | 1056.01 | 441.27 | 3048.27 | 932.21 |
| | | CEPT | 150 | 221.87 | 71.87 | 5324.89 | 95.21 | 1029.48 | 1124.69 | 663.98 | 3036.79 | 943.69 |
| | | | 250 | 250.00 | 0.00 | 5330.92 | 0.00 | 1013.95 | 1013.95 | 642.24 | 3040.22 | 940.26 |
| | | | 350 | 315.93 | 0.00 | 5343.91 | 0.00 | 999.19 | 999.19 | 407.93 | 3047.63 | 932.85 |
| S2 | Base Case Policy | | – | 864.00 | – | 14655.38 | 0.00 | 2950.57 | – | – | 8357.96 | – |
| | ON/ OFF | CP | – | 570.50 | – | 11109.12 | 114.29 | 2090.10 | 2204.39 | 919.27 | 6335.53 | 2022.43 |
| | | CPaEPT | 400 | 492.00 | 92.00 | 11089.63 | 135.43 | 2133.35 | 2268.77 | 1040.80 | 6324.41 | 2033.55 |
| | | | 550 | 557.50 | 7.50 | 11098.88 | 114.69 | 2098.54 | 2213.23 | 1036.24 | 6329.69 | 2028.27 |
| | | | 700 | 579.50 | 0.00 | 11125.38 | 116.09 | 2090.57 | 2206.67 | 924.21 | 6344.80 | 2013.16 |
| | | CEPT | 400 | 471.50 | 71.50 | 11085.12 | 94.72 | 2139.30 | 2234.02 | 1331.26 | 6321.85 | 2036.11 |
| | | | 550 | 550.00 | 0.00 | 11094.62 | 0.00 | 2097.01 | 2097.01 | 1269.55 | 6327.26 | 2030.70 |
| | | | 700 | 698.50 | 0.00 | 11111.88 | 0.00 | 2089.56 | 2089.56 | 861.01 | 6337.10 | 2020.86 |
| | FPC | CP | – | 572.39 | – | 10974.74 | 114.67 | 2058.42 | 2173.09 | 950.57 | 6258.89 | 2099.07 |
| | | CPaEPT | 400 | 470.41 | 70.41 | 10930.97 | 122.45 | 2103.99 | 2226.44 | 1083.13 | 6233.93 | 2124.03 |
| | | | 550 | 550.00 | 0.00 | 10962.93 | 110.18 | 2067.92 | 2178.10 | 1071.37 | 6252.16 | 2105.80 |
| | | | 700 | 572.37 | 0.00 | 10974.60 | 114.67 | 2058.40 | 2173.07 | 957.81 | 6258.82 | 2099.14 |
| | | CEPT | 400 | 455.66 | 55.66 | 10935.74 | 73.73 | 2114.24 | 2187.98 | 1377.30 | 6236.66 | 2121.31 |
| | | | 550 | 550.00 | 0.00 | 10958.31 | 0.00 | 2066.91 | 2066.91 | 1299.65 | 6249.53 | 2108.43 |
| | | | 700 | 700.00 | 0.00 | 10969.35 | 0.00 | 2057.65 | 2057.65 | 892.92 | 6255.82 | 2102.14 |

(*continued*).

**Table 4.** Continued.

| | Charging scheme | Costing method | $P^{thr}$ (kW) | $p_{peak}$ (kW) | $\Delta P^{+}$ (kW) | Energy (kWh) | cost (SGD) | | | | Carbon emission (kg) | |
|---|---|---|---|---|---|---|---|---|---|---|---|---|
| | | | | | | | Peak | Energy | Total | Saving | Total | Reduction |
| S3 | Base Case Policy | | – | 2290.50 | – | 38914.38 | 0.00 | 7831.85 | – | – | 22192.87 | – |
| | ON/OFF | CP | – | 1702.50 | – | 29871.12 | 341.07 | 5536.43 | 5877.49 | 2413.22 | 17035.50 | 5157.37 |
| | | CPaEPT | 1000 | 1298.00 | 298.00 | 29785.38 | 379.43 | 5759.58 | 6139.01 | 2668.76 | 16986.60 | 5206.27 |
| | | | 1500 | 1505.50 | 5.50 | 29867.63 | 303.81 | 5654.20 | 5958.00 | 2649.44 | 17033.51 | 5159.36 |
| | | | 2000 | 1703.50 | 0.00 | 29882.38 | 341.27 | 5549.26 | 5890.53 | 2121.62 | 17041.92 | 5150.95 |
| | | CEPT | 1000 | 1260.50 | 260.50 | 29769.87 | 345.11 | 5764.71 | 6109.82 | 3431.68 | 16977.76 | 5215.11 |
| | | | 1500 | 1500.00 | 0.00 | 29758.62 | 0.00 | 5621.26 | 5621.26 | 3257.85 | 16971.34 | 5221.52 |
| | | | 2000 | 1988.50 | 0.00 | 29875.37 | 0.00 | 5532.14 | 5532.14 | 2299.71 | 17037.93 | 5154.94 |
| | FPC | CP | – | 1717.11 | – | 29526.96 | 343.99 | 5448.73 | 5792.73 | 2497.99 | 16839.23 | 5353.64 |
| | | CPaEPT | 1000 | 1252.90 | 252.90 | 29355.28 | 352.33 | 5661.35 | 6013.67 | 2794.10 | 16741.31 | 5451.55 |
| | | | 1500 | 1500.00 | 0.00 | 29421.85 | 300.50 | 5542.56 | 5843.06 | 2764.38 | 16779.28 | 5413.59 |
| | | | 2000 | 1717.11 | 0.00 | 29526.97 | 343.99 | 5448.73 | 5792.73 | 2219.42 | 16839.23 | 5353.64 |
| | | CEPT | 1000 | 1224.79 | 224.79 | 29367.11 | 297.80 | 5679.13 | 5976.93 | 3564.57 | 16748.06 | 5444.81 |
| | | | 1500 | 1500.00 | 0.00 | 29421.84 | 0.00 | 5542.56 | 5542.56 | 3336.55 | 16779.28 | 5413.59 |
| | | | 2000 | 2000.00 | 0.00 | 29515.49 | 0.00 | 5447.13 | 5447.13 | 2384.73 | 16832.68 | 5360.19 |
| S4 | Base Case Policy | | – | 3277.50 | – | 52588.75 | 0.00 | 10606.31 | – | – | 29991.36 | – |
| | ON/OFF | CP | – | 2086.50 | – | 40083.75 | 418.00 | 7526.73 | 7944.73 | 3318.17 | 22859.76 | 7131.60 |
| | | CPaEPT | 1500 | 1766.00 | 266.00 | 40028.25 | 460.37 | 7716.65 | 8177.01 | 3798.07 | 22828.11 | 7163.25 |
| | | | 2000 | 2004.00 | 4.00 | 40166.25 | 403.07 | 7598.51 | 8001.58 | 3773.17 | 22906.81 | 7084.55 |
| | | | 3000 | 2083.00 | 0.00 | 40101.50 | 417.29 | 7540.70 | 7957.99 | 2828.61 | 22869.89 | 7121.48 |
| | | CEPT | 1500 | 1705.00 | 205.00 | 40084.75 | 271.58 | 7746.27 | 8017.86 | 4943.28 | 22860.33 | 7131.03 |
| | | | 2000 | 2000.00 | 0.00 | 40041.75 | 0.00 | 7562.06 | 7562.06 | 4736.68 | 22835.81 | 7155.55 |
| | | | 3000 | 2847.50 | 0.00 | 40086.00 | 0.00 | 7513.05 | 7513.05 | 3093.26 | 22861.05 | 7130.32 |
| | FPC | CP | – | 2092.38 | – | 39532.99 | 419.17 | 7395.09 | 7814.26 | 3448.64 | 22545.66 | 7445.70 |
| | | CPaEPT | 1500 | 1717.82 | 217.82 | 39362.99 | 431.41 | 7561.37 | 7992.78 | 3982.30 | 22448.71 | 7542.65 |
| | | | 2000 | 2000.00 | 0.00 | 39478.26 | 400.67 | 7432.93 | 7833.60 | 3941.15 | 22514.45 | 7476.91 |
| | | | 3000 | 2092.38 | 0.00 | 39533.00 | 419.17 | 7395.09 | 7814.26 | 2972.34 | 22545.67 | 7445.69 |
| | | CEPT | 1500 | 1641.09 | 141.09 | 39386.24 | 186.92 | 7614.67 | 7801.59 | 5159.54 | 22461.97 | 7529.39 |
| | | | 2000 | 2000.00 | 0.00 | 39478.24 | 0.00 | 7432.93 | 7432.93 | 4865.81 | 22514.44 | 7476.92 |
| | | | 3000 | 2863.45 | 0.00 | 39534.37 | 0.00 | 7395.69 | 7395.69 | 3210.61 | 22546.45 | 7444.91 |

showcases substantial cost savings and environmental benefits.

In terms of port operation costs, we quantify the cost savings of the S1–S4 instances compared to the base case. The FPC scheme achieves a maximum daily cost saving of 663.98, 1377.30, 3564.57, and 5159.54 SGD/day, for 100, 250, 500, and 1000 reefers, respectively. The ON/OFF charging scheme delivers a maximum cost saving of 645.02, 1331.26, 3431.68, and 4943.28 SGD/day. These reductions in operational costs offer significant financial benefits to port operators, enabling them to improve efficiency and profitability while optimising resource utilisation.

Furthermore, from the perspective of energy conservation and emission reduction, the suggested methods reduce energy consumption by approximately 1615, 3675, 9275, and 12,810 kWh/day for S1–S4 compared to the base case in average. The energy saving leads to a decrease in carbon emissions, with the FPC scheme reducing emissions by 945.14, 2124.03, 5451.55, and 7542.65 kg/day, while the ON/OFF charging scheme achieves a reduction of 910.06, 2036.11, 5221.52, and 7163.25 kg/day for S1–S4 instances. The total annual reduction in energy could reach up to approximately 590, 1340, 3385, and 4675 MWh/day, with corresponding carbon emission reductions of around 338, 760, 1950, and 2684 tons/year for S1–S4 instances, respectively. These reductions provide significant environmental benefits by lowering the carbon footprint and promoting sustainable practices in port operations.

For two smart charging control schemes of reefers, the FPC scheme outperforms the ON/OFF charging scheme. Specifically, the FPC reefers achieve daily reductions in energy demand of approximately 58 kWh, 144 kWh, 382, and 552 kWh; energy costs of 12 SGD, 30 SGD, 92, and 117 SGD; and carbon emissions of 33 kg, 82 kg, 218, and 315 kg in average, compared to the ON/OFF scheme, for S1–S4 instances, respectively. In summary, the FPC scheme offers greater load flexibility, enabling more efficient energy management compared to the ON/OFF scheme.

The three different peak costing methods (CP, CPaEPT, and CEPT) have had a significant impact on both cost and environmental outcomes, though the effects vary slightly across methods. The total cost of the CEPT method is lowest when the peak power remains below the threshold. In contrast, the total cost of the CP method is minimised when the peak power exceeds the threshold. Meanwhile, the total cost of the CPaEPT method is consistently the highest, regardless of the peak power level. When the peak power does not reach the threshold, the total cost of the CPaEPT method is nearly the same as that of the CP method. Our research provides valuable insights for port operators in making strategic decisions, particularly in selecting a peak power costing method and determining the peak threshold values in contracts with power suppliers (grid operators).

In summary, the demand response mechanism, which shifts power demand to lower-cost periods, proves to be effective, with consistent results across ports of varying sizes. The methods proposed in this research offer a practical solution for optimising port operations through smart charging management, resulting in both cost savings and environmental benefits. This study contributes to the advancement of more sustainable and economically viable practices in port operations.

#### 5.2.3. Energy peak-shaving and demand response with different charging schemes and peak costing

Figures 7–9 illustrate the total power charging amount in each hour across different charging schemes and peak threshold values. FPC and ON/OFF fixed power charging schemes have been presented with subfigures for S2 and S3 instances as examples. Within each subfigure, the results are provided for three peak costing methods (CP, CPaEPT, and CEPT), as well as the base case policy and the always-on fixed power approach.

When comparing the two smart charging schemes (FPC and ON/OFF) with the Base Case Policy and the Always-On Fixed Power Policy, the two smart charging schemes show better performance as they optimise the timing of charging power. Their demand response is effectively managed through charging flexibility based on time-of-use energy price. Energy consumption is shifted to the early hours of the day, when energy prices are lower. As a result, electricity consumption is reduced during the day, particularly between 7 AM and 3 PM. The shift in power demand is a key component of the demand response mechanism, driven mainly by the time-of-use energy prices, which are higher between 7 AM and 10 PM, as shown in Figure 6. Meanwhile, within the limitations of the peak threshold for the CEPT method, a higher peak threshold value (Figure 9) allows a greater gain in demand response, particularly by allowing more reefer containers to be powered simultaneously during periods of lower energy prices.

There are also some differences between the FPC and ON/OFF smart charging schemes in terms of peak-shaving and demand response results. The flexibility of the FPC scheme is higher compared to that of the ON/OFF scheme, which leads to less fluctuation in power demand. This reduced fluctuation is particularly beneficial for the capacitated power distribution network, as it helps to stabilise power flow and maintain infrastructure reliability.

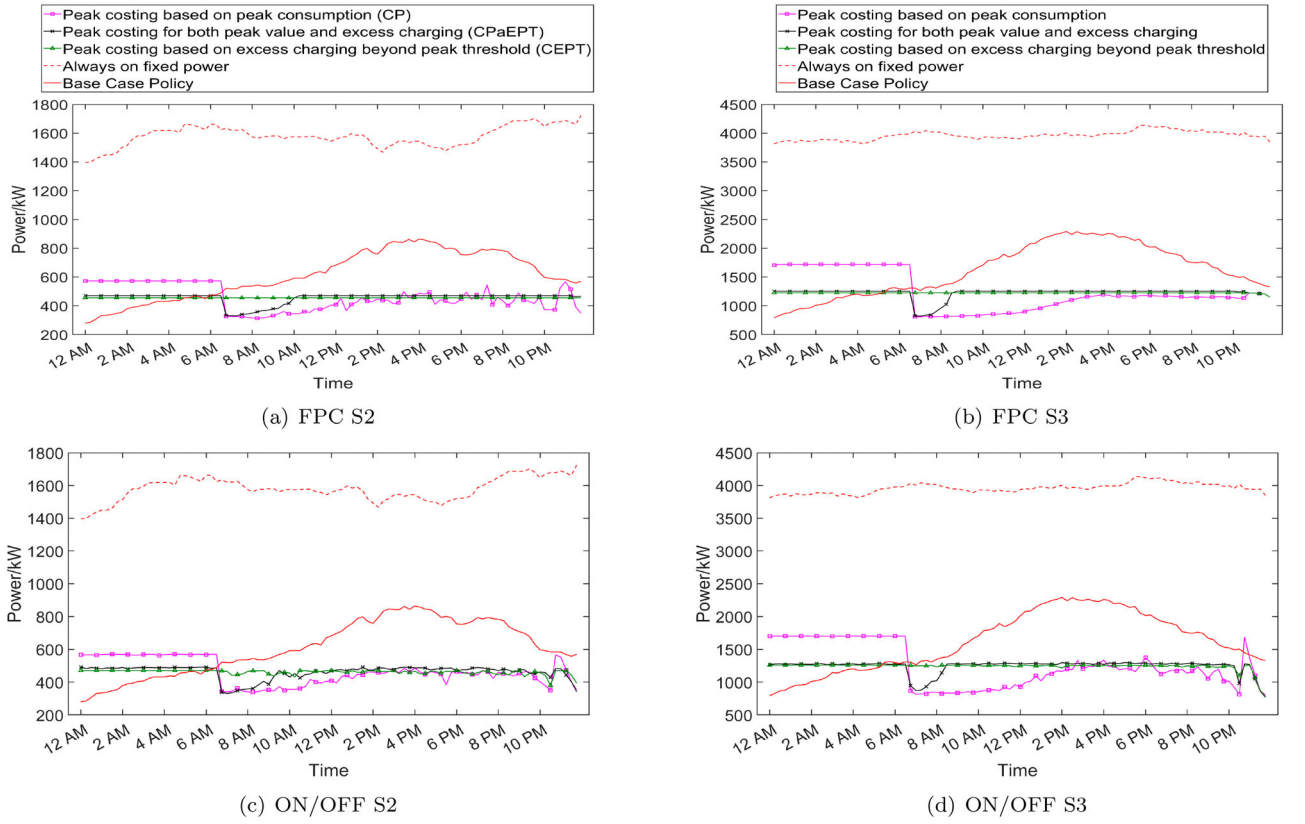


**Figure 7.** Power charging with low peak threshold. (a) FPC S2. (b) FPC S3. (c) ON/OFF S2 and (d) ON/OFF S3.

By comparing the results from low, medium, and high peak thresholds, it clearly shows that the peak threshold significantly affect the amount of power that can be shifted to lower-cost energy periods, particularly in the CEPT and CPaEPT methods. For S1–S4 instances, CP method is not affected by the threshold value, with its peak power consistently remaining at approximately 282.5 kW, 570.5 kW, 1702.5 kW, and 2086.5 kW for ON/OFF scheme, as well as 282.76 kW, 572.39 kW, 1717.11 kW, and 2092.38 kW for FPC scheme. In the CEPT case, the primary goal is to minimise power consumption that exceeds the peak threshold. As a result, the peak power is kept close to the threshold, allowing as much power as possible to be shifted to lower-cost energy periods, thereby reducing overall energy costs. However, if the peak threshold is set too high (Figure 9), the peak may not be reached due to the limitations of the power distribution network's capacity. On the other hand, if the threshold is set too low (Figure 7), the power curve will flatten out, staying as close to the threshold as possible. This phenomenon is desirable in this case, as the price of peak power is significantly higher than the hourly energy prices. It demonstrates the effectiveness of the optimisation strategy in shifting power consumption and highlights the strong responsiveness of case CEPT in various peak thresholds. In the CPaEPT case with a low peak threshold (Figure 7), the peak power is minimised to stay as close to the threshold as possible. But it's slightly higher than that of the CEPT case and the power curve forms a dip between 7 AM and 11 AM. In case CPaEPT with high peak thresholds, the peak power is nearly the same as that of case CP, as shown in Figure 9. For medium peak thresholds, as shown in Figure 8, the power curve closely mirrors that of the CEPT case, with the peak power equal to the threshold. Case CPaEPT demonstrates a nuanced performance in managing peak power across different peak thresholds. It is capable of significant peak power reduction and optimising energy use under stringent conditions with low and medium peak thresholds. The CPaEPT's response to high thresholds is less effective than that of the CEPT.

#### 5.2.4. Analysis of reefer charging rate with different peak threshold values

Figure 10 illustrates the hourly charging rate of reefer containers at the yard, using the S2 instance as an example. It includes both FPC and ON/OFF charging schemes across different peak threshold settings. In contrast to the Base Case policy, all the smart charging optimisation scenarios incorporate some form of demand response by shifting charging to lower energy price periods.

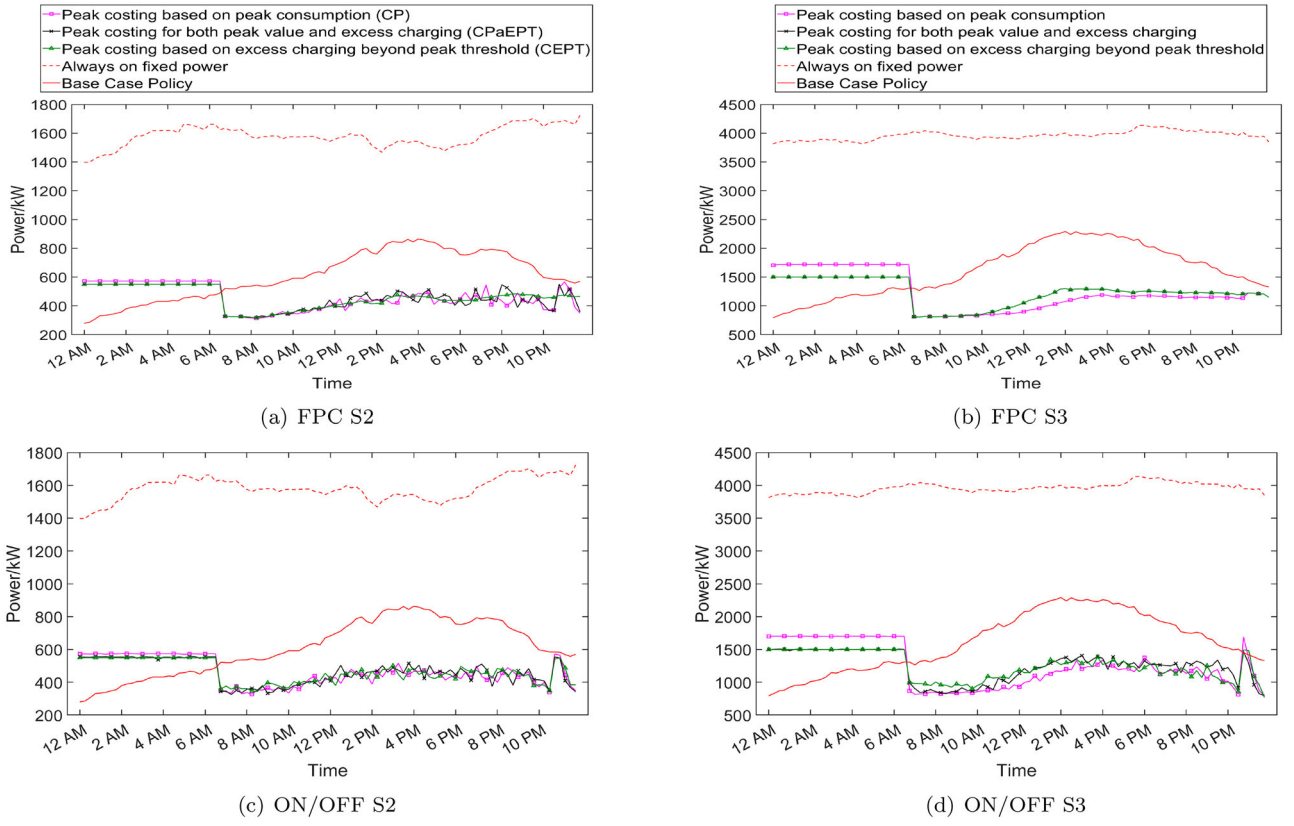


**Figure 8.** Power charging with medium peak threshold. (a) FPC S2. (b) FPC S3. (c) ON/OFF S2 and (d) ON/OFF S3.

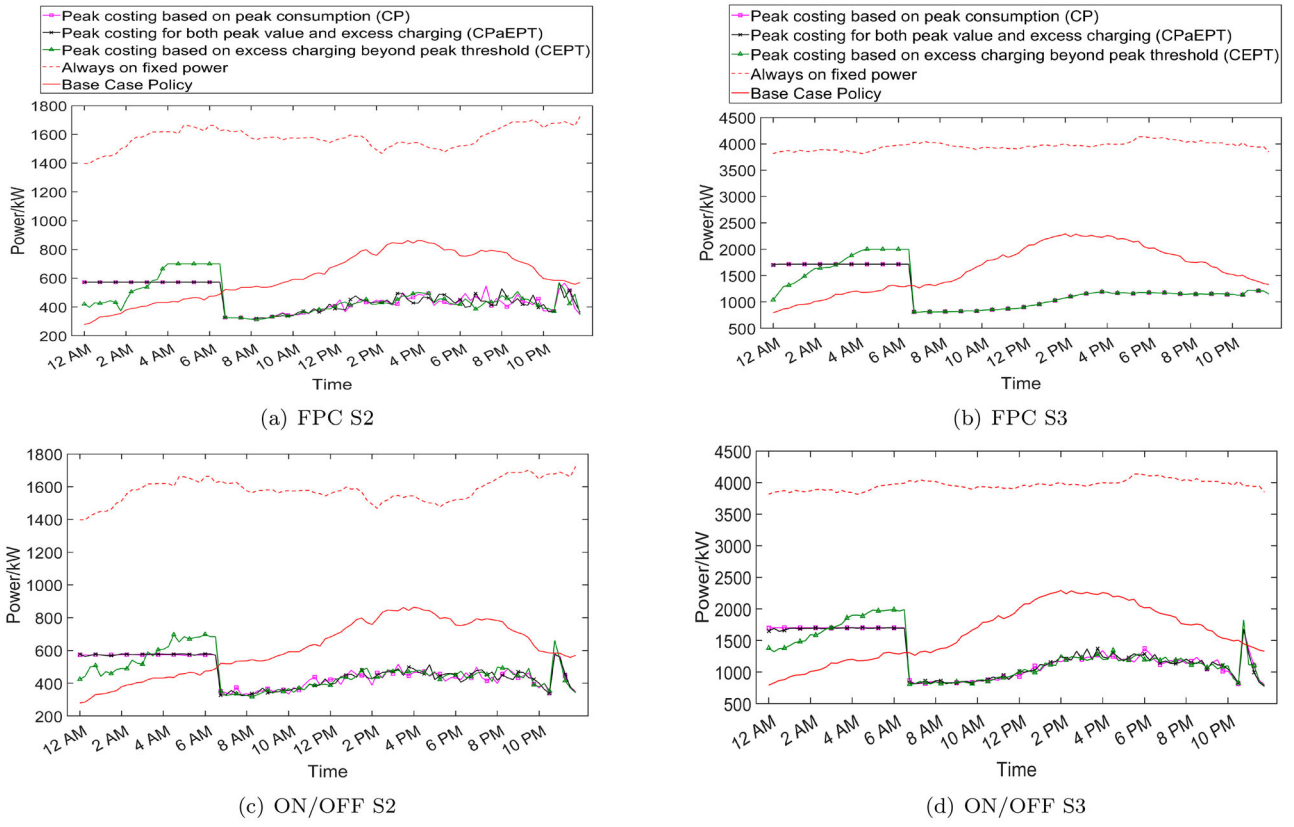


**Figure 9.** Power charging with high peak threshold. (a) FPC S2. (b) FPC S3. (c) ON/OFF S2 and (d) ON/OFF S3.

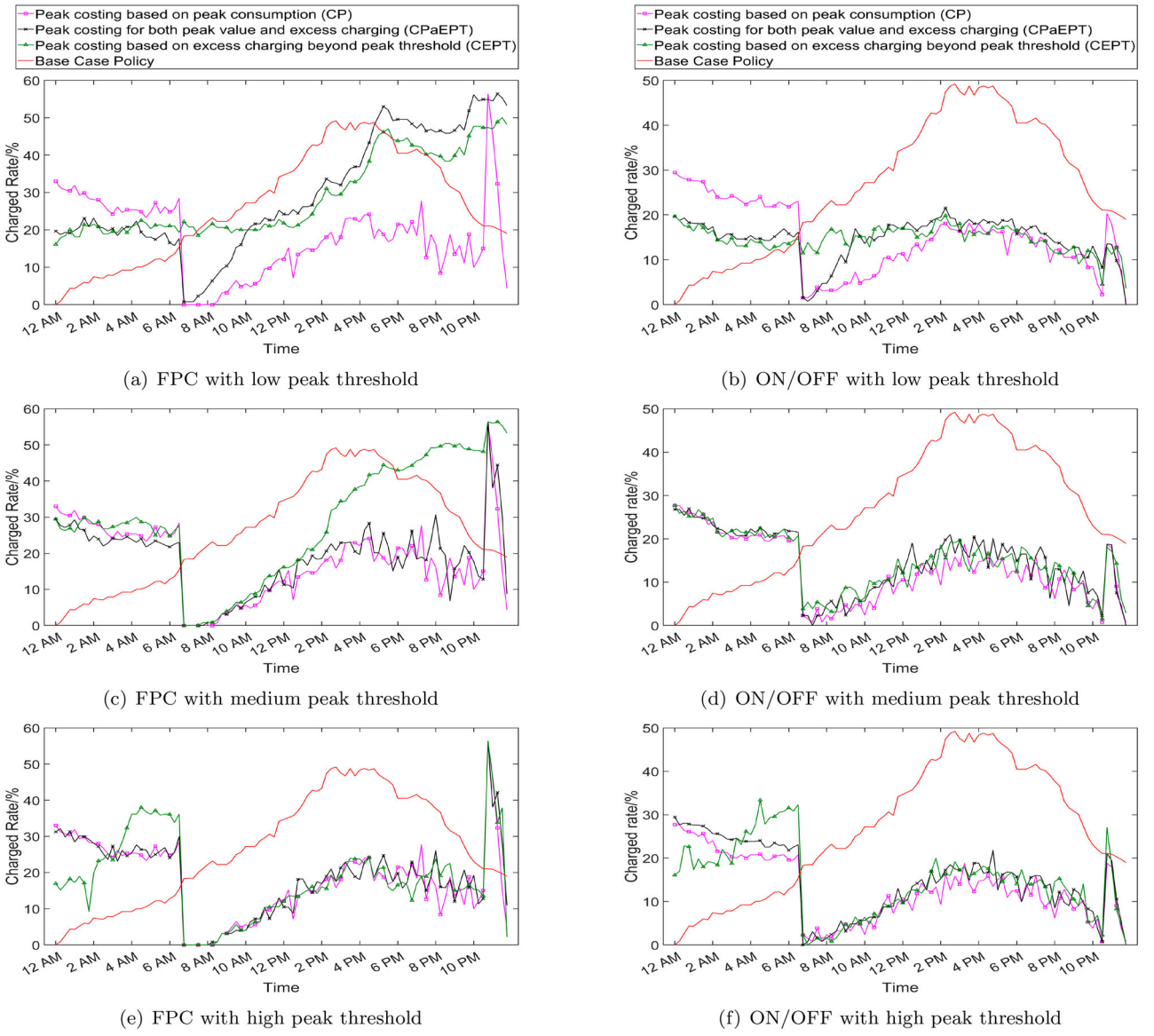


**Figure 10.** Charging rate of S2 instance. (a) FPC with low peak threshold. (b) ON/OFF with low peak threshold. (c) FPC with medium peak threshold. (d) ON/OFF with medium peak threshold. (e) FPC with high peak threshold and (f) ON/OFF with high peak threshold.

As shown in Figure 10(a–d), the FPC smart charging scheme using the CEPT method with low and medium peak thresholds, as well as the CPaEPT method with the low peak threshold, exhibits a steady increase starting from 7 AM. This trend differs from that of the ON/OFF charging scheme. Due to the low and medium peak threshold, their charging rate is distributed more evenly throughout the entire day. For high peak threshold, the FPC scheme consistently achieves a higher charging rate than the ON/OFF scheme before 7 AM. This is due to the greater flexibility in power management offered by the FPC scheme. As a result, with the same total power supplied by the yard, more reefers can be charged under the FPC scheme.

Figure 11 illustrates this trend through the temperature and power plots for two reefers (Frozen reefer and Chilled reefer) as examples. FPC control provides a continuous supply of moderate power to maintain the temperature within the allowed limits. This approach enables more reefers to be charged during this period, whereas the ON/OFF control relies on intermittent maximum cooling power, leading to more fluctuating charging behaviour.

### 5.2.5. Temperature management for reefer containers

Figure 12 shows the average internal temperature , along with the minimum and maximum allowable

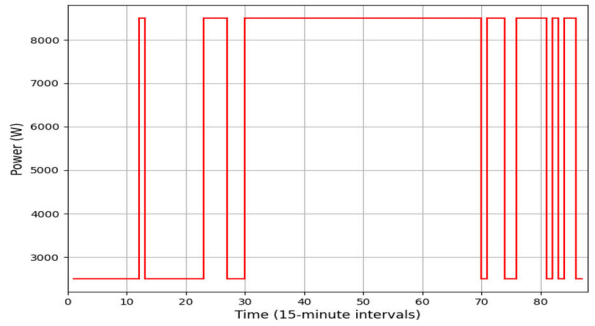


(a) ON/OFF power-Frozen reefer

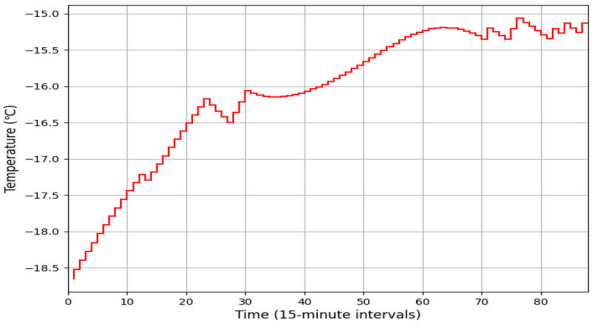


(b) ON/OFF temp-Frozen reefer

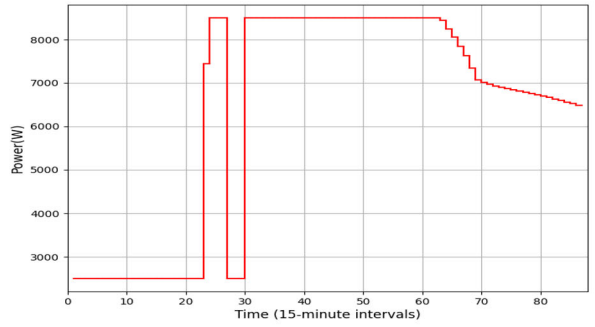


(c) FPC power-Frozen reefer

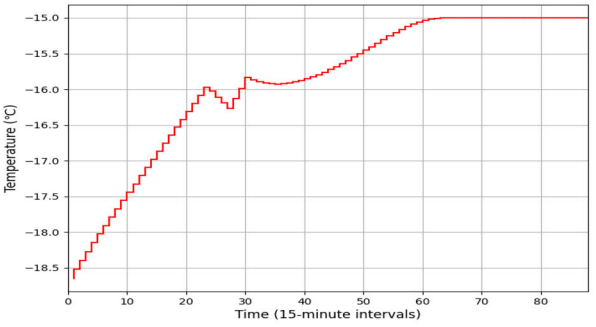


(d) FPC temp-Frozen reefer

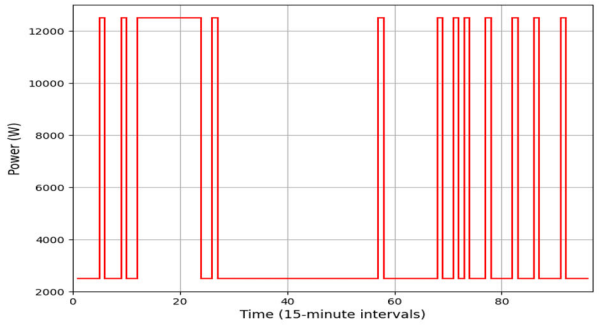


(e) ON/OFF power-Chilled reefer

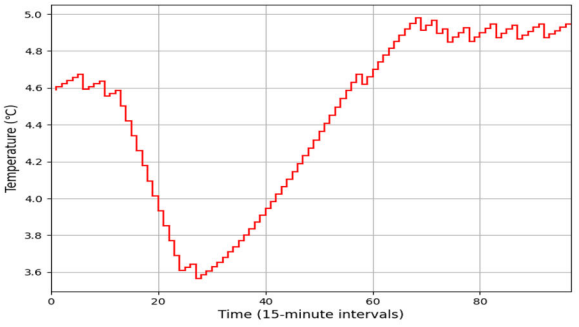


(f) ON/OFF temp-Chilled reefer

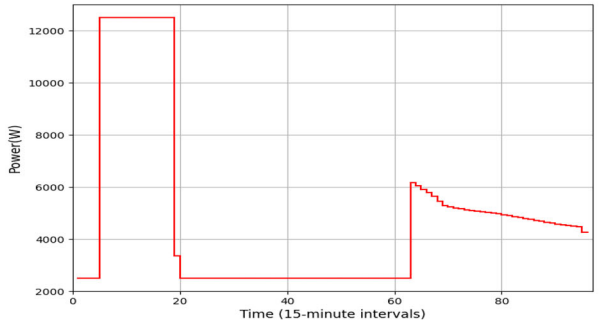


(g) FPC power-Chilled reefer

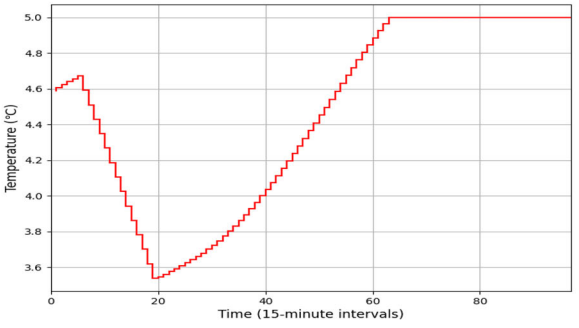


(h) FPC temp-Chilled reefer

**Figure 11.** An illustration of temperature and power charging curve for two reefers in the benchmark. (a) ON/OFF power-Frozen reefer. (b) ON/OFF temp-Frozen reefer. (c) FPC power-Frozen reefer. (d) FPC temp-Frozen reefer. (e) ON/OFF power-Chilled reefer. (f) ON/OFF temp-Chilled reefer. (g) FPC power-Chilled reefer and (h) FPC temp-Chilled reefer.

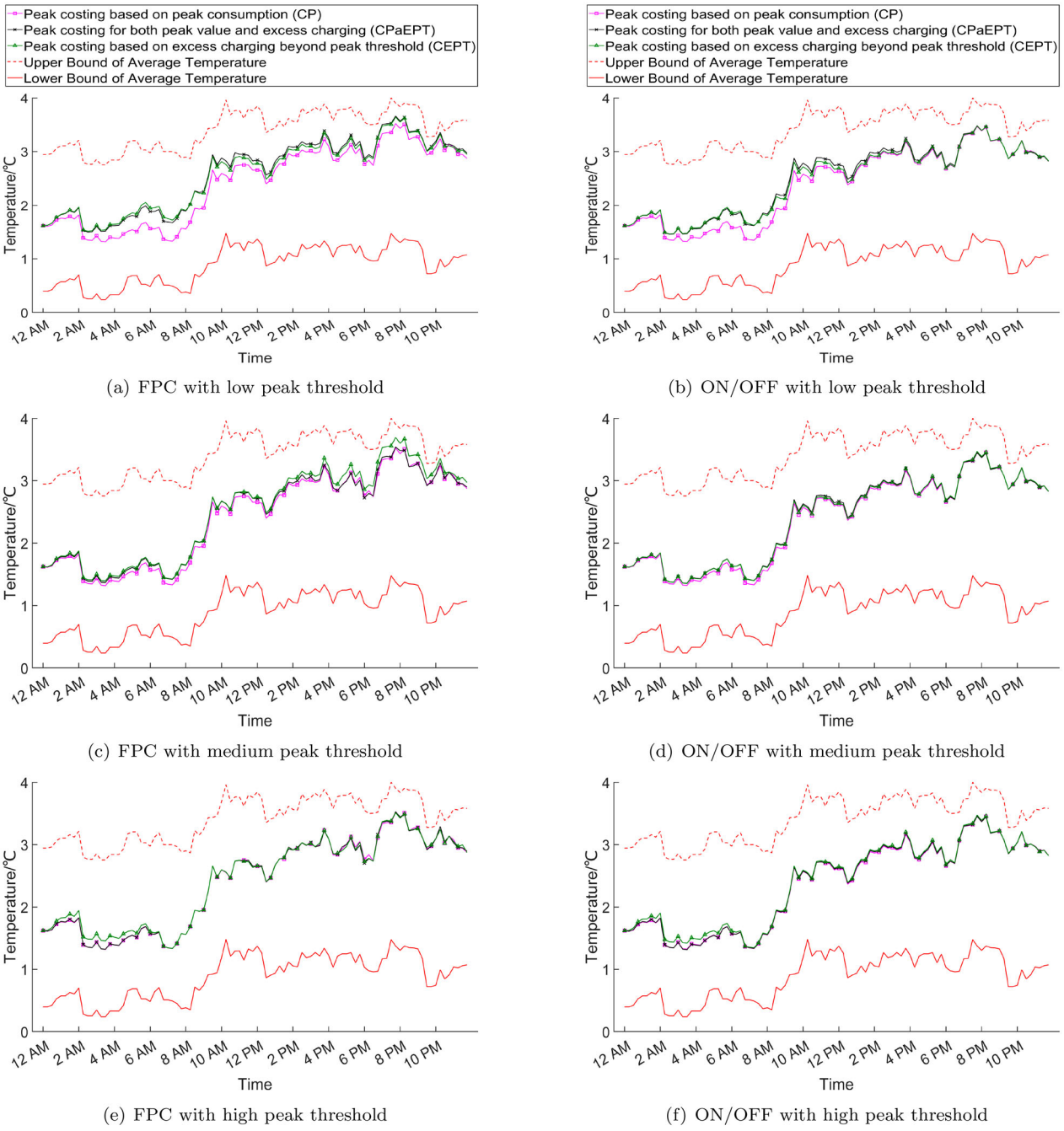


**Figure 12.** Average temperature of S2 instance. (a) FPC with low peak threshold. (b) ON/OFF with low peak threshold. (c) FPC with medium peak threshold. (d) ON/OFF with medium peak threshold. (e) FPC with high peak threshold and (f) ON/OFF with high peak threshold.

temperatures of all reefers for different charging schemes with three thresholds in S2 instance. The proposed method ensures that all reefers remain within the desired temperature range. The average temperatures for the FPC and ON/OFF charging schemes are relatively similar for a given instance. Furthermore, when comparing different peak-costing approaches (CP, CPaEPT, and CEPT) for the same instance in each sub-figure, the results show little variation. The charging power and average temperature are inversely proportional across all three peak-costing methods, with higher charging power leading to lower average temperatures. Results indicate that the average temperature from 11 AM to 10 PM is close to the upper allowed limit. During this period, the ambient temperature and sun intensity are high, as well as demand response mechanism carefully shifts power charging to other periods in order to reduce unit energy purchasing costs. At night (12 AM – 8 AM), the average temperature

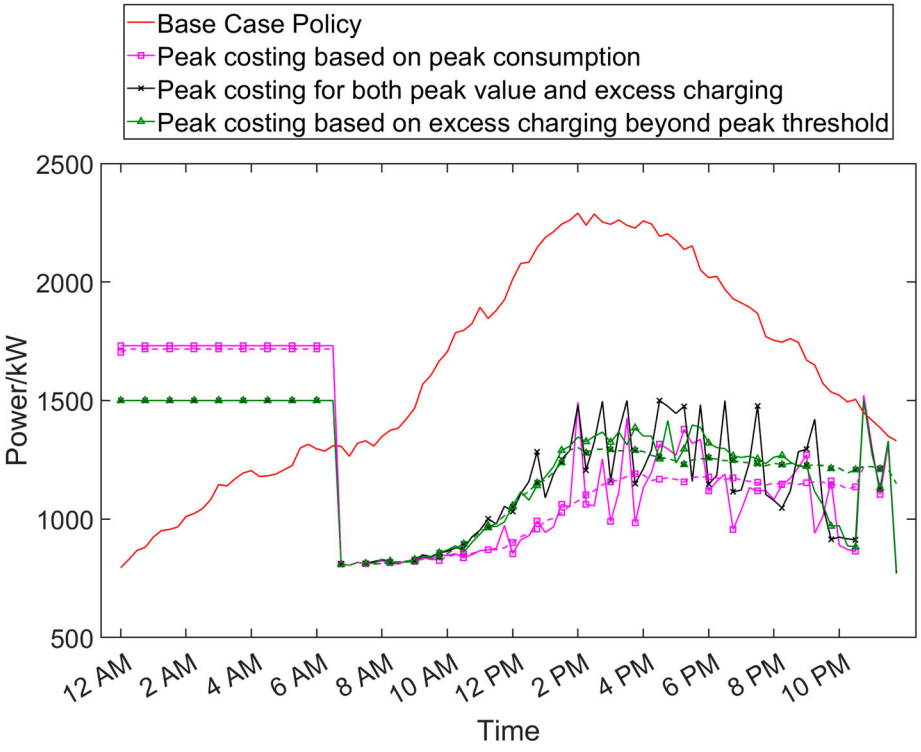


**Figure 13.** Power charging with and without power distribution network for S3 instance.

for reefer containers falls within the range between the lower and upper temperature limits.

### 5.3. The impact of power distribution network in the yard

Figure 13 illustrates an example of power charging comparing both with and without a power distribution network for S3 instance. The solid lines represent the results without the power distribution network, while the dashed lines correspond to the S3 instance with the network in place. It is evident that the power distribution network helps to reduce fluctuations between 7 AM and 10 PM. Without the network limitation, charging is primarily influenced by time-of-use energy pricing and the peak threshold costing. However, since the energy price remains constant and below the threshold between 7 AM and 10 PM, there is no mechanism in place to restrict power consumption during these hours. In contrast, the power distribution network divides the reefers stored in the yard into multiple groups, balancing load distribution across different nodes. This prevents overloading at any single nodes in Figure 3 and ensures a more stable power supply throughout the day. As a result, the presence of the power distribution network leads to a more stable and reliable charging experience, particularly during the critical hours between 7 AM and 10 PM when energy demand is below peak power.

Figures 7–9 illustrate that both S1 and S2 show fluctuations between 7 AM and 10 PM when the power distribution network is in place. This is because the number of reefers is relatively small, and the capacity of the network nodes is not fully utilised. Only when the number of refrigerated containers is significantly larger (S3 and S4 instances), the effect of the power distribution network becomes more apparent.

### 5.4. Installation of roof shade (RS) in the yard

Installing roof shades over the reefer area is a critical topic of discussion in the port industry. Roof shades have a solar radiation absorption rate of 50% (Shinoda, Budiyanto, and Sugimura 2022), which is expected to enhance energy efficiency in reefer yards. An alternative approach is the construction of underground storage and cooling spaces for reefer containers (Moros-Daza et al. 2024). This study evaluates the potential benefits of installing a roof shade in the yard. We have set the environmental parameters with the roof shade, as shown in Figure 14, and conducted experiments with S2 instance.

#### 5.4.1. The impact analysis of roof shade on charging schemes

Table 5 presents the peak power and energy demand for the RS case, as well as the differences between scenarios with and without the roof shade (RS and S2 instances).

**Table 5.** Peak power and energy demand for RS and the differences between scenarios with and without roof shade (RS and S2).

| | | | RS | | | Reduction only by roof shade | | |
|---|---|---|---|---|---|---|---|---|
| Smart charging scheme | Peak costing method | $P^{thr}$ (kW) | $p_{peak}$ (kW) | $\Delta P^{+}$ (kW) | Total energy demand (kWh) | $p_{peak}$ (kW) | $\Delta P^{+}$ (kW) | Total energy demand (kWh) |
| Base Case Policy with roof shade | | – | 823.00 | – | 13955.13 | 41.00 | – | 700.25 |
| ON/OFF | CP | – | 543.50 | – | 10486.62 | 27.00 | – | 622.50 |
| | CPaEPT | 400 | 461.50 | 61.50 | 10465.38 | 30.50 | 30.50 | 624.25 |
| | | 550 | 546.50 | 0.00 | 10489.13 | 11.00 | 7.50 | 609.75 |
| | | 700 | 547.00 | 0.00 | 10489.63 | 32.50 | 0.00 | 635.75 |
| | CEPT | 400 | 441.50 | 41.50 | 10458.87 | 30.00 | 30.00 | 626.25 |
| | | 550 | 550.00 | 0.00 | 10482.12 | 0.00 | 0.00 | 612.50 |
| | | 700 | 688.50 | 0.00 | 10479.63 | 10.00 | 0.00 | 632.25 |
| FPC | CP | – | 543.38 | – | 10355.02 | 29.01 | – | 619.72 |
| | CPaEPT | 400 | 455.40 | 55.40 | 10314.63 | 15.02 | 15.02 | 616.34 |
| | | 550 | 543.36 | 0.00 | 10354.71 | 6.64 | 0.00 | 608.22 |
| | | 700 | 543.37 | 0.00 | 10355.17 | 29.00 | 0.00 | 619.43 |
| | CEPT | 400 | 429.94 | 29.94 | 10318.61 | 25.71 | 25.71 | 617.14 |
| | | 550 | 550.00 | 0.00 | 10354.90 | 0.00 | 0.00 | 603.41 |
| | | 700 | 700.00 | 0.00 | 10349.47 | 0.00 | 0.00 | 619.88 |

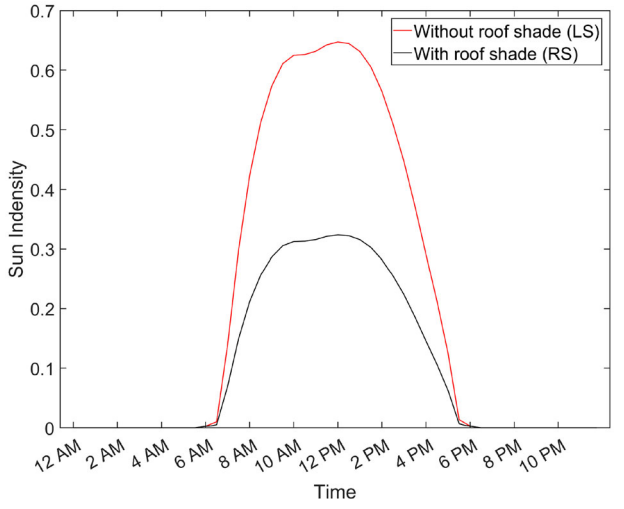


**Figure 14.** Sun intensity with/without roof shade.

The results show that installing the roof shade reduces total energy demand, peak energy consumption, and the peak demand exceeding the threshold in both charging schemes and three peak costing methods. The installation of the roof shade can reduce peak power by up to 30 kW and save more than 600 kWh/day in total energy consumption.

### *5.4.2. The impact of roof shade on cost and environmental performance*

Table 6 outlines the various cost components (Peak costs, Energy costs, Total costs) and carbon emissions for roof shade (RS) case, as well as reduction in cost and carbon thanks to roof shade compared to the base case policy with/without roof shade and the optimisation without roof shade for S2 instance. Results demonstrate positive impact of RS on costs and carbon emissions. For all RS cases, the total costs range from 1937.24 to 2131.54 SGD/day, and the carbon emissions range from 5882.44 to 5982.23 kg/day. The FPC schemes generally result in lower energy consumption (and emissions) as well as reduced total costs compared to the ON/OFF schemes with RS.

Table 6 also presents the cost savings and carbon emission reductions for peak costing optimisation methods compared to the Base Case Policy with roof shade. In particular, the various peak costing schemes still show significant reductions in both energy costs and carbon emissions with roof shade. A smaller threshold (400 kW) provides greater cost savings compared to higher thresholds (550 and 700 kW) in the CEPT and CPaEPT cases when roof shading is installed. This lower threshold better presents the performance of roof shading.

Compared to the base case with roof shade, the FPC scheme achieves a maximum cost savings of 1319.83 SGD/day and a reduction in carbon emissions of 2076.17 kg/day. The ON/OFF charging scheme, on the other hand, results in a maximum cost savings of 1280.08 SGD/day and a reduction in carbon emissions of 1993.91 kg/day. These average savings could total approximately 475,000 SGD/year, with a potential reduction in carbon emissions of up to 740 tons/year for the S2 instance with roof shade, compared to the Base Case Policy. In terms of both energy cost and carbon emission reductions, the FPC scheme outperforms the ON/OFF charging scheme.

Table 6 details the impact of roof shade installation compared each optimisation result between RS instance and S2 instance shown in Table 4. The total cost savings range from 120.41 to 159.67 SGD/day, while carbon emissions are reduced by 344.12 to 362.57 kg/day. These savings could amount to approximately 51,000 SGD/year and 129 tons/year. This data clearly demonstrates the positive effect of roof shading in reducing energy demand, energy costs, and carbon

**Table 6.** Cost and carbon emissions for RS instances and the reduction by peak costing optimisation and roof shade.

| Charging scheme | Peak costing method | $p^{thr}$ (kW) | Peak costs (SGD) | Energy costs (SGD) | Total costs (SGD) | Carbon emission (kg) | Reduction only by peak costing optimisation | | Reduction only by roof shade | | Reduction by both roof shade and peak costing optimisation | |
|---|---|---|---|---|---|---|---|---|---|---|---|---|
| | | | | | | | Cost (SGD) | Carbon (kg) | Cost (SGD) | Carbon (kg) | Cost (SGD) | Carbon (kg) |
| ON/OFF | CP | – | 108.88 | 1968.08 | 2076.96 | 5980.52 | 881.95 | 1978.09 | 127.43 | 355.01 | 1046.70 | 2377.44 |
| | CPaEPT | 400 | 117.09 | 2014.44 | 2131.54 | 5968.40 | 996.86 | 1990.20 | 137.24 | 356.01 | 1178.03 | 2389.56 |
| | | 550 | 109.48 | 1968.19 | 2077.67 | 5981.95 | 990.62 | 1976.66 | 135.56 | 347.74 | 1171.80 | 2376.01 |
| | | 700 | 109.58 | 1968.34 | 2077.92 | 5982.23 | 896.42 | 1976.37 | 128.75 | 362.57 | 1052.95 | 2375.73 |
| | CEPT | 400 | 54.98 | 2019.37 | 2074.35 | 5964.70 | 1280.08 | 1993.91 | 159.67 | 357.15 | 1490.93 | 2393.26 |
| | | 550 | 0.00 | 1967.17 | 1967.17 | 5977.96 | 1188.54 | 1980.65 | 129.84 | 349.31 | 1399.39 | 2380.00 |
| | | 700 | 0.00 | 1966.98 | 1966.98 | 5976.53 | 827.06 | 1982.08 | 122.59 | 360.57 | 983.60 | 2381.43 |
| FPC | CP | – | 108.86 | 1938.01 | 2046.86 | 5905.47 | 912.05 | 2053.14 | 126.23 | 353.42 | 1076.80 | 2452.49 |
| | CPaEPT | 400 | 113.43 | 1977.77 | 2091.19 | 5882.44 | 1037.20 | 2076.17 | 135.25 | 351.50 | 1218.38 | 2475.52 |
| | | 550 | 108.85 | 1937.95 | 2046.80 | 5905.29 | 1021.49 | 2053.31 | 131.30 | 346.87 | 1202.67 | 2452.67 |
| | | 550 | 108.85 | 1937.95 | 2046.80 | 5905.29 | 1021.49 | 2053.31 | 131.30 | 346.87 | 1083.97 | 2452.40 |
| | CEPT | 400 | 39.67 | 1994.93 | 2034.60 | 5884.70 | 1319.83 | 2073.90 | 153.38 | 351.95 | 1530.68 | 2473.26 |
| | | 550 | 0.00 | 1938.02 | 1938.02 | 5905.40 | 1217.69 | 2053.21 | 128.89 | 344.12 | 1428.54 | 2452.56 |
| | | 700 | 0.00 | 1937.24 | 1937.24 | 5902.30 | 856.80 | 2056.31 | 120.41 | 353.52 | 1013.34 | 2455.66 |

emissions. The installation of roof shade offers an efficient and sustainable solution for energy management.

In comparison to the base case policy without roof shade of the S2 instance, the combined impact of roof shade and peak costing optimisation is presented in Table 6. The total cost savings range from 983.60 to 1530.68 SGD per day, while carbon emissions are reduced by 2375.73 to 2475.52 kg per day. The effect of roof shading and peak costing optimisation results in more substantial cost reductions and efficiency gains than either strategy could achieve individually.

## 6. Conclusion

Our study focuses on the smart charging planning of reefers for energy demand response and energy peak-shaving at ports using Internet-of-Things (IoT) technology. By leveraging intermittent charging capabilities and responsiveness to time-variant energy prices, we optimise power charging and temperature management during each time period of the planning horizon. Addressing the challenges posed by the increasing electrification of ports, our research provides effective strategies for reducing energy costs, mitigating peak energy stress on the grid, and reducing the carbon emissions associated with charging. We consider the diverse attributes of reefers, such as dynamic arrival/departure times and reefer cargo content requirements, as well as external factors like ambient temperature and sunlight intensity and power distribution network properties, to deliver comprehensive insights.

The suggested operational policies building Cyber-Physical Systems (CPS) for an Internet-of-Things (IoT) framework transform traditional reefers into smart reefers within Industry 4.0. This integration forms an interconnected network that enables seamless communication among reefers and enhances real-time monitoring, data collection, and power control. The optimisation models embedded in this IoT framework provide decisions on power and temperature control for energy peak load shaving and demand response management. Given the flexibility of IoT-based control, two types of smart reefer charging methods (FPC and ON/OFF charging) and three energy costing methods (including different types of peak costs and total energy consumption costs) are investigated. The suggested CPS enable suggested charging schemes.

Results show that the power charging for reefers can effectively be shifted between periods and intermittent charging is helpful, reducing electricity consumption, peak power purchasing and total energy costs. The power charging is shifted to early hours of the day, influenced by high energy prices during the day. The power charging is

also carefully distributed between periods to limit peak power consumption as the unit peak power consumption cost is higher compared to the average unit power consumption cost per period. Our study also informs ports about different energy costing schemes (e.g. unit energy consumption and energy peak costing). Three different peak costing schemes are evaluated in this work. For the schemes with peak costing beyond the peak threshold, the value of agreed peak thresholds plays a crucial role in managing power consumption effectively. A high peak threshold may lead to energy waste, while a low threshold could restrict power shifting (demand response) and incur high peak costs and energy consumption costs. The power distribution network leads to a more stable and reliable charging experience for larger-scale reefer yards, such as S3 and S4 instances, particularly during the critical hours between 7 AM and 10 PM when energy demand is below peak power. Moreover, roof shading has been identified as an efficient method for decreasing the power demand during daytime hours (and resulting costs and emissions), reducing the need for a demand response.

We also compare two smart charging schemes. Our study suggests that flexible power charging (FPC) control delivers better performance compared to ON/OFF charging control with respect to studied costs and constraints. FPC control leads to a smoother power consumption curve and maintains a more consistent temperature within the reefers. In contrast, ON/OFF control frequently cycles between maximum and minimum power states, causing more frequent temperature fluctuations and increased wear on refrigeration equipment. The enhanced flexibility of FPC control results in more efficient energy use, greater cost savings, and better preservation of goods. Additionally, the model for FPC scheme is easier to solve and we obtain optimal solutions within short computational times (less than 3 seconds).

Our research quantifies the substantial cost savings and environmental benefits of smart charging mechanisms and roof shade installation. The total annual reduction in energy could reach up to approximately 590, 1340, 3385, and 4675 MWh/day, with corresponding carbon emission reductions of around 338, 760, 1950, and 2684 tons/year for S1–S4 instances. These annual cost savings could reach to approximately 240,000, 500,000, 1,270,000, and 1,850,000 SGD/year. Roof shade could save total cost more approximately 51,000 SGD/year and reduce carbon emission more 129 tons/year than S2 instance.

The managerial implications of our work offer port operators the means to make informed decisions on electricity supplier contracts (selecting a proper costing structure), peak threshold decisions, and power charging amounts in each time period. In addition to reducing energy costs, this approach helps to minimise product spoilage and ensure the quality, freshness, and safety of cargo in the cold chain. Through effective energy and temperature management, we also reduce the environmental impact of refrigerated container transportation, making this technology more sustainable and eco-friendly. While this work considers the application of reefer containers at container terminals and yards, the proposed approach may equally be applied to related problems in logistics and storage of refrigerated goods.

It is important to also acknowledge the limitations of our study. Our research solely focuses on reefer park in a container terminal. However, a complete energy management system in a port would include other energy consumers such as container transport and handling equipment. Future works can integrate other energy demand generators into refining the optimisation models, and additional factors such as specific cargo requirements can be integrated in the models. Furthermore, exact and heuristic solution algorithms can be studied to enhance the optimality performance of the solution approaches. In future studies, the reefers can capture more data with sensors (e.g. humidity) and forecast their temperature with machine learning methods. These data can serve as input for our charging optimisation platform. IoT systems require robust security measures. Blockchain can manage access and secure communications and transactions by the cryptography layer (Surucu-Balci, Iris, and Balci 2024). Thus, future research could also focus on enhancing the security of IoT-enabled reefers through blockchain that will also deliver a secure platform for electric power supply contracts.

## Disclosure statement

No potential conflict of interest was reported by the author(s).

## Notes on contributors

*Dr Guolei Tang* is an Associate Professor at Dalian University of Technology.

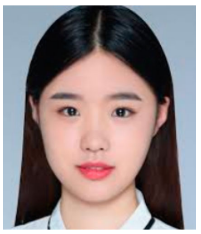

*Ms Zhuoyao Zhao* is a PhD student at Dalian University of Technology.

*Dr Frederik Schulte* is an Assistant Professor at Delft University of Technology.

*Dr Çağatay Iris* is an Associate Professor at the University of Liverpool. He is the corresponding author of the article.

## Data availability statement

The data that support the findings of this study are available from the corresponding author upon reasonable request.

## ORCID

*Frederik Schulte* http://orcid.org/0000-0003-3159-4393
*Çağatay Iris* http://orcid.org/0000-0001-5422-354X

## References

Alasali, Feras, Stephen Haben, and William Holderbaum. March, 2019. "Energy Management Systems for a Network of Electrified Cranes with Energy Storage." *International Journal of Electrical Power & Energy Systems* 106:210–222. https://doi.org/10.1016/j.ijepes.2018.10.001.

Alghamdi, Turki G., Dhaou Said, and Hussein T. Mouftah. 2021. "Profit Maximization for Evses-Based Renewable Energy Sources in Smart Cities with Different Arrival Rate Scenarios." *IEEE Access* 9:58740–58754. https://doi.org/10.1109/ACCESS.2021.3070485.

Aloqaily, Osama I., Irfan Al-Anbagi, Dhaou Said, and Hussein T. Mouftah. 2016. "Flexible Charging and Discharging Algorithm for Electric Vehicles in Smart Grid Environment." In *IEEE Wireless Communications and Networking Conference (WCNC 2016) – Track 4 – Services, Applications, and Business*, 1–6. Doha, Qatar: IEEE. https://doi.org/10.1109/WCNC.2016.7565123.

Budiyanto, Muhammad Arif, Nasruddin Ir, and Fariz Zhafari. 2019. "Simulation Study Using Building-Design Energy Analysis to Estimate Energy Consumption of Refrigerated Container." *Energy Procedia* 156:207–211. https://doi.org/10.1016/j.egypro.2018.11.129.

Budiyanto, Muhammad Arif, Firman Ady Nugroho, B. Wibowo, and Takeshi Shinoda. 2018. "Estimated of Energy saving from the Application of Roof Shade on the Refrigerated Container Storage Yard." *Journal of Advanced Research in Fluid Mechanics and Thermal Sciences* 46:114–121. https://semarakilmu.com.my/journals/index.php/fluid_mechanics_thermal_sciences/article/view/2745

Budiyanto, Muhammad Arif, and Takeshi Shinoda. 2017. "Stack Effect on Power Consumption of Refrigerated Containers in Storage Yards." *International Journal of Technology* 8:1182. https://doi.org/10.14716/ijtech.v8i7.771.

Charpentier, Vincent, Nina Slamnik-Kriještorac, Giada Landi, Matthias Caenepeel, Olivier Vasseur, and Johann M. Marquez-Barja. 2024. "Paving the Way Towards Safer and More Efficient Maritime Industry with 5g and beyond Edge Computing Systems." *Computer Networks* 250:110499. https://doi.org/10.1016/j.comnet.2024.110499.

Geerlings, Harry, Robert Heij, and Ron van Duin. 2018. "Opportunities for Peak Shaving the Energy Demand of Ship-To-Shore Quay Cranes at Container Terminals." *Journal of Shipping and Trade* 3 (1): 3. https://doi.org/10.1186/s41072-018-0029-y.

International Institute of Refrigeration. 2022. "Reefer Container Throughput in Main European Ports." Accessed February 14, 2025. https://iifiir.org/en/news/reefer-container-throughput-in-main-european-ports.

Iris, çağatay, and Jasmine Siu Lee Lam. 2019. "A Review of Energy Efficiency in Ports: Operational Strategies, Technologies and Energy Management Systems." *Renewable and Sustainable Energy Reviews* 112:170–182. https://doi.org/10.1016/j.rser.2019.04.069.

Iris, çağatay, and Jasmine Siu Lee Lam. 2021. "Optimal Energy Management and Operations Planning in Seaports with Smart Grid While Harnessing Renewable Energy under Uncertainty." *Omega* 103:102445. https://doi.org/10.1016/j.omega.2021.102445.

Jiao, Zihao, Ying Yin, Lun Ran, and Zhen Gao. 2022. "Integrating Vehicle-To-grid Contract Design with Power Dispatching Optimisation: Managerial Insights, and Carbon Footprints Mitigation." *International Journal of Production Research* 60 (17): 5354–5379. https://doi.org/10.1080/00207543.2021.1956694.

Khabbouchi, Imed, Dhaou Said, Aziz Oukaira, Idir Mellal, and Lyes Khoukhi. 2023. "Machine Learning and Game-Theoretic Model for Advanced Wind Energy Management Protocol (awemp)." *Energies* 16 (5): 2179. https://doi.org/10.3390/en16052179.

Lu, Ying, Sidun Fang, Tao Niu, and Ruijin Liao. 2023. "Energy-Transport Scheduling for Green Vehicles in Seaport Areas: A Review on Operation Models." *Renewable and Sustainable Energy Reviews* 184:113443. https://doi.org/10.1016/j.rser.2023.113443.

Mao, Anjia, Tiantian Yu, Zhaohao Ding, Sidun Fang, Jinran Guo, and Qianqian Sheng. 2022. "Optimal Scheduling for Seaport Integrated Energy System considering Flexible Berth Allocation." *Applied Energy* 308:118386. https://doi.org/10.1016/j.apenergy.2021.118386.

Moros-Daza, Adriana, Dariela Castro, Jose Bonifacio, Rene Amaya-Mier, and Stefan Voß. 2024. "Greening Container Terminals: An Innovative and Cost-Effective Solution for Sustainable Reefer Container Storage." *Journal of Cleaner*

*Production* 466:142664. https://doi.org/10.1016/j.jclepro.2024.142664.

Munusamy, Nagarajan, and Indragandhi Vairavasundaram. 2024. "Ai and Machine Learning in V2g Technology: A Review of Bi-Directional Converters, Charging Systems, and Control Strategies for Smart Grid Integration." *e-Prime – Advances in Electrical Engineering, Electronics and Energy* 10:100856. https://doi.org/10.1016/j.prime.2024.100856.

Nel, Margot, Leila Louise Goedhals-Gerber, and Esbeth van Dyk. 2024. "A Comparison of Different Technologies to Improve Temperature Control in Refrigerated Containers: A Table Grape Export Case." *Heliyon* 10 (4): e25988. https://doi.org/10.1016/j.heliyon.2024.e25988.

Port of Antwerp. 2025. "Deepsea Terminals in Antwerp." Online Resource. Accessed February 15, 2025. https://www.portofantwerpbruges.com/en/deepsea-terminals.

Port Of Rotterdam. 2021. "Container Terminals and Depots in the Port of Rotterdam." Accessed December 15, 2024. https://www.portofrotterdam.com/sites/default/files/2021-06/container-terminals-and-depots-in-the-rotterdam-port-area.pdf.

Port Technology International. 2021. "Hongkong International Terminals Launches Greater Bay's Largest Remote Reefer Monitoring System." Accessed February 20, 2025. https://www.porttechnology.org/news/hongkong-international-terminals-launches-greater-bays-largest-remote-reefer-monitoring-system/.

Prabhu, Vittaldas V., Damien Trentesaux, and Marco Taisch. 2015. "Energy-Aware Manufacturing Operations." *International Journal of Production Research* 53 (23): 6994–7004. https://doi.org/10.1080/00207543.2015.1100766.

PSA International. 2018. "Cold Phain – Keeping It Cool." Accessed February 14, 2025. https://www.globalpsa.com/cold-chain-keeping-cool/.

Said, Dhaou. 2023. "A Survey on Information Communication Technologies in Modern Demand-Side Management for Smart Grids: Challenges, Solutions, and Opportunities." *IEEE Engineering Management Review* 51 (1): 76–107. https://doi.org/10.1109/EMR.2022.3186154.

Said, Dhaou, and Hussein T. Mouftah. 2017. "A Novel Electric Vehicles Charging/Discharging Scheme with Load Management Protocol." In *Conference Proceedings: IEEE ICC 2017 SAC Symposium Communications for the Smart Grid Track*, 1–6. Dresden, Germany: IEEE. https://doi.org/10.1109/ICC.2017.7997117.

Said, Dhaou, Mubashir Husain Rehmani, Idir Mellal, Aziz Oukaira, and Ahmed Lakhssass. 2024. "Cybersecurity Based on Converged form of Blockchain, Internet-of-Things and Machine Learning in Smart Micro-Grid." In *2024 International Conference on Computing, Internet of Things and Microwave Systems (ICCIMS)*, Quebec, Canada, 1–6. https://doi.org/10.1109/ICCIMS61672.2024.10690628.

Sarantakos, Ilias, Saman Nikkhah, Meltem Peker, Annabel Bowkett, Timur Sayfutdinov, Arman Alahyari, Charalampos Patsios, et al. 2024. "A Robust Logistics-Electric Framework for Optimal Power Management of Electrified Ports under Uncertain Vessel Arrival Time." *Cleaner Logistics and Supply Chain* 10:100144. https://doi.org/10.1016/j.clscn.2024.100144.

Sarda, Jigar, Nilay Patel, Hirva Patel, Rohan Vaghela, Biswajit Brahma, Akash Kumar Bhoi, and Paolo Barsocchi. 2024. "A Review of the Electric Vehicle Charging Technology, Impact on Grid Integration, Policy Consequences, Challenges and Future Trends." *Energy Reports* 12:5671–5692. https://doi.org/10.1016/j.egyr.2024.11.047.

Shinoda, Takeshi, Muhammad Arif Budiyanto, and Yoshihisa Sugimura. 2022. "Analysis of Energy Conservation by Roof Shade Installations in Refrigerated Container Areas." *Journal of Cleaner Production* 377:134402. https://doi.org/10.1016/j.jclepro.2022.134402.

Surucu-Balci, Ebru, çağatay Iris, and Gökcay Balci. 2024. "Digital Information in Maritime Supply Chains with Blockchain and Cloud Platforms: Supply Chain Capabilities, Barriers, and Research Opportunities." *Technological Forecasting and Social Change* 198:122978. https://doi.org/10.1016/j.techfore.2023.122978.

Tang, Guolei, Ming Qin, Zhuoyao Zhao, Jingjing Yu, and Chen Shen. 2020. "Performance of Peak Shaving Policies for Quay Cranes at Container Terminals with Double Cycling." *Simulation Modelling Practice and Theory* 104:102129. https://doi.org/10.1016/j.simpat.2020.102129.

van Duin, J. H. R. (Ron), H. (Harry) Geerlings, A. (Alexander) Verbraeck, and T. (Tushar) Nafde. 2018. "Cooling down: A Simulation Approach to Reduce Energy Peaks of Reefers at Terminals." *Journal of Cleaner Production* 193:72–86. https://doi.org/10.1016/j.jclepro.2018.04.258.

Wang, Yucong, and Ping Chen. 2024. "An Adaptive Large Neighbourhood Search for Multi-Depot Electric Vehicle Routing Problem with Time Windows." *European Journal of Industrial Engineering* 18 (4): 606–636. https://doi.org/10.1504/EJIE.2024.139327.

Xiong, Chang, Yixin Su, Hao Wang, Danhong Zhang, and Binyu Xiong. 2024. "Optimal Distributed Energy Scheduling for Port Microgrid System considering the Coupling of Renewable Energy and Demand." *Sustainable Energy, Grids and Networks* 39:101506. https://doi.org/10.1016/j.segan.2024.101506.

Zhang, Bo, Meng Zhao, and Xiangpei Hu. 2023. "Location Planning of Electric Vehicle Charging Station with Users' Preferences and Waiting Time: Multi-Objective Bi-Level Programming Model and Hnsga-Ii Algorithm." *International Journal of Production Research* 61 (5): 1394–1423. https://doi.org/10.1080/00207543.2021.2023832.